



TECHNICAL UNIVERSITY OF LIBEREC
Faculty of Mechatronics, Informatics
and Interdisciplinary Studies ■

CREATION AND DEVELOPMENT OF SOFT COMPUTING MODELS FOR USE IN NUCLEAR ENGINEERING

Diploma thesis

Study programme: N2612 – Electrical Engineering and Informatics

Study branch: 3906T001 – Mechatronics

Author: **Bc. Jakub Hořeňovský**

Supervisor: prof. Dr. Ing. Alexander Kratzsch



DIPLOMA THESIS ASSIGNMENT

(PROJECT, ART WORK, ART PERFORMANCE)

First name and surname: **Bc. Jakub Hořeňovský**
Study program: **N2612 Electrical Engineering and Informatics**
Identification number: **M11000303**
Specialization: **Mechatronics**
Topic name: **Creation and Development of Soft Computing Models for use in Nuclear Engineering**
Assigning department: **Institute of Mechatronics and Computer Engineering**

R u l e s f o r e l a b o r a t i o n :

1. Survey of available literature (research on the state of art)
2. Choosing of an appropriate simulation tool
3. Choosing of suitable Soft Computing Methods and definition of requirements for experiments
4. Development of simulation models of Soft Computing Methods
5. Evaluation of the model quality
6. A further development of Soft Computing Methods in terms of their dynamics and sensitivity
7. Documentation of the results

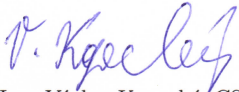


Scope of graphic works: **In respect to the documentation needs**
Scope of work report
(scope of dissertation): **c. 40–50 pages**
Form of dissertation elaboration: **printed/electronical**
Language of dissertation elaboration: **English**
List of specialized literature:

- [1] **P. Hoffman, "Current knowledge on core degradation phenomena, a review," Journal of Nuclear Materials, Nr. 270, pp. 194-211, 6 November 1999.**
- [2] **V. Slugeň, Safety of VVER-440 Reactors - Barriers Againsts Fission Products Release, London: Springer, 2011.**
- [3] **L. A. Zadeh, "Fuzzy Sets," Information and Control, pp. 338-353, 30 November 1965.**
- [4] **C.-C. Wong and C.-C. Chen, "A Clustering-Based Method for Fuzzy Modeling," IEICE Trans. Inf. a Syst., Vols. E82-D, no. 6, pp. 1058-1065, june 1999.**

Tutor for dissertation: **prof. Dr. Ing. Alexander Kratzsch**
Hochschule Zittau/Görlitz
Dissertation Counsellor: **Dipl.-Ing. Sebastian Schmidt**
Hochschule Zittau/Görlitz, IPM

Date of dissertation assignment: **1 September 2013**
Date of dissertation submission: **16 May 2014**


prof. Ing. Václav Kopecký, CSc.
Dean




doc. Ing. Milan Kolář, CSc.
Department Manager

Liberec, dated: 1 September 2013

Declaration

I hereby certify that I have been informed the Act 121/2000, the Copyright Act of the Czech Republic, namely § 60 - Schoolwork, applies to my master thesis in full scope.

I acknowledge that the Technical University of Liberec (TUL) does not infringe my copyrights by using my master thesis for TUL's internal purposes.

I am aware of my obligation to inform TUL on having used or licensed to use my master thesis; in such a case TUL may require compensation of costs spent on creating the work at up to their actual amount.

I have written my master thesis myself using literature listed therein and consulting it with my thesis supervisor and my tutor.

Concurrently I confirm that the printed version of my master thesis is coincident with an electronic version, inserted into the IS STAG.

Date:

Signature:

Abstract

The development of gamma distribution around the reactor vessel during the meltdown has been postulated, starting with normal operation state and ending with core material relocation into the lower plenum of the RPV. Based on data representing the γ -distribution, soft computing models (MLP, fuzzy models by Mamdani and by Takagi-Sugeno-Kang) are developed in this thesis. Quality analysis of the models is evaluated based on error characteristics, internal parameters (where applicable) and random values. The best-choice models of each type are chosen according to their quality, and a sensitivity analysis for cases of various input failures is performed. All findings are summarized and measures for the improvement of the models behavior are suggested.

Keywords:

Pressurized water reactors, Soft Computing methods, MLP, fuzzy models, quality analysis

Abstrakt

Bylo postulováno rozložení intenzit gama záření kolem jaderného reaktoru během procesu tavení jádra. Na základě dat, reprezentujících rozložení gama záření pro stavy od standardní operace až po přesun roztaveného jaderného materiálu do spodní oblasti tlakovodního reaktoru, jsou v této práci vyvinuty a popsány „Soft Computing“ modely (vícevrstvý perceptron, fuzzy model podle Mamdaniho a podle Takagi-Sugeno-Kanga). Kvalita modelů je vyhodnocena prostřednictvím chybových charakteristik, vnitřních parametrů modelů (vhodných typů) a analýzy pomocí náhodných čísel. Těmito metodami jsou vybrány nejvhodnější modely každého typu. U nich je provedena analýza citlivosti pro různé varianty poruch na vstupech. Na závěr jsou shrnuty výsledky a předloženy návrhy pro zlepšení chování modelů.

Klíčová slova:

Tlakovodní reaktory, metody Soft Computing, MLP, fuzzy modely, analýza kvality

Table of Contents

Abstract	4
Abstrakt	5
Table of Contents	6
List of Figures	9
List of Tables	12
List of Abbreviations and Symbols	14
1 Introduction	16
1.1 Position of the work.....	16
1.2 Objective of the work	17
1.3 Structure of the work	17
2 General Basics	19
2.1 Pressurized Water Reactors	19
2.1.1 Design and Functionality	19
2.1.2 Safety Systems.....	21
2.1.3 Radioactive Inventory in the Reactor Coolant System.....	21
2.1.4 Barriers of Fission Products	22
2.2 Core Meltdown in PWR	23
2.2.1 Initiating events	24
2.2.2 Early In-Vessel Phase	24
2.2.3 Late In-Vessel Phase	27
2.2.4 Gamma distribution for the low-pressure scenario.....	28
2.3 Soft Computing Methods.....	31
2.3.1 Fuzzy Systems by Mamdani.....	31
2.3.1.1 Membership functions	31
2.3.1.2 Fuzzy rules.....	32
2.3.1.3 Methods of operators	34
2.3.1.4 Example – ‘Tipper’	35
2.3.2 Fuzzy Systems by Takagi-Sugeno-Kang.....	36
2.3.2.1 TSK-Systems with the Cluster Algorithm by Wong and Chen.....	37
2.3.3 Multilayer Perceptrons	40
2.3.3.1 Neuron transfer function.....	41

2.3.3.2	Training of MLP	42
2.3.3.3	Backpropagation	43
2.3.3.4	Test and recall.....	44
3	Methods for quality evaluation of FM-, TSK- and MLP-models.....	45
3.1	Model quality analysis based on error values.....	45
3.2	Model quality analysis based on internal parameters	46
3.2.1	Weight analysis of a MLP model	46
3.2.2	Correlation analysis of a TSK-model	48
3.3	Model quality analysis based on random numbers.....	48
4	Development of models	49
4.1	Description of datasets.....	50
4.1.1	Training and test datasets	51
4.1.2	Recall datasets for validation of SCMs	55
4.2	Error limits and decision criteria for the investigations	55
4.3	Development of fuzzy model by Mamdani (FM).....	56
4.3.1	Quality analysis of FM model	58
4.4	Development of MLP models.....	62
4.4.1	Weight analysis of MLP models	63
4.4.2	Quality analysis of MLP models based on random values.....	67
4.5	Development of TSK models	69
4.5.1	TSK models by not normalized data	69
4.5.1.1	Correlation analysis of TSK n.n. models.....	70
4.5.1.2	Analysis of TSK n.n. model based on random values.....	72
4.5.2	TSK models by normalized data	73
4.5.2.1	Correlation analysis of TSK n. models.....	74
4.5.2.2	Analysis of TSK n. model based on random values.....	75
4.6	Comparison of models.....	76
5	Sensitivity analysis of the models	78
5.1	General method of sensitivity analysis	78
5.2	Results of sensitivity analysis using zero inputs	79
5.2.1	Fuzzy model by Mamdani	80
5.2.2	MLP models	81
5.2.3	TSK models	83
5.3	Results of sensitivity analysis using random inputs	84

5.3.1	Fuzzy model by Mamdani	86
5.3.2	MLP models	87
5.3.3	TSK models	88
5.4	Summary of sensitivity analysis.....	89
5.5	Recommendations based on sensitivity analysis	90
6	Conclusion	91
	References.....	94
	Appendix A – Training data	96
	Appendix B – Test data	97
	Appendix C – Data-CD.....	98

List of Figures

Figure 1-1: Schematic principle of measurement for detection of core meltdown (side view of RPV)	16
Figure 2-1: Schema of Pressurized Water Reactor (PWR) [5].....	20
Figure 2-2: Significant core states during core meltdown in LWR [1]	26
Figure 2-3: Postulated gamma distribution based on core states from figure 2-2 [1]	30
Figure 2-4: Standard membership functions.....	32
Figure 2-5: Typical arrangement of membership functions of a fuzzy variable	33
Figure 2-6: Schema of a fuzzy system by Mamdani [16].....	33
Figure 2-7: Rule diagram of example system ‘Tipper’	36
Figure 2-8: Schema of a fuzzy system by Takagi-Sugeno-Kang [16].....	37
Figure 2-9: Division of dataset with input and output data into clusters [18]	37
Figure 2-10: Schema of a TSK model with the cluster algorithm by Wong and Chen [18]	39
Figure 2-11: Block diagram of design of TSK-model with the cluster algorithm by Wong and Chen [18].....	40
Figure 2-12: General structure of an artificial neural network	41
Figure 2-13: Illustration of backward propagation of error	43
Figure 3-1: Examples of correlation factors [18]	46
Figure 4-1: Schema of general method for investigations.....	49
Figure 4-2: 3-D plot of training dataset produced based on postulated core states during core meltdown.....	52
Figure 4-3: Graphical interpretation of data from table 4-4	54
Figure 4-4: Graphical illustration of training (blue) and test (red) datasets	55
Figure 4-5: Membership functions of input no. 15.....	57
Figure 4-6: Graphical representation of data from table 4-5 (training errors of the FM model)	58
Figure 4-7: Graphical representation of data from table 4-6 (test errors of the FM model)	59
Figure 4-8: Analysis of FM model based on random values (recall data 1) – all input vectors are classified as state 9.	60
Figure 4-9: Analysis of FM model based on random values (recall data 2) – all input vectors are classified as state 9.	60

Figure 4-10: Analysis of FM model based on random values (recall data 3) – model correctly classifies most of the input vectors	61
Figure 4-11: Comparison of FM model outputs and original states used for generation of random values	61
Figure 4-12: Analysis of MLP model no. 7 based on random values (recall data 3). The color of line determines index of the input vector – the first one green, the last one blue; the RGB value changes linearly	67
Figure 4-13: Comparison of MLP model no. 7 outputs and original states used for generation of random values	67
Figure 4-14: Analysis of MLP model no. 12 based on random values (recall data 3)	68
Figure 4-15: Comparison of MLP model no. 12 outputs and original states used for generation of random values	68
Figure 4-16: Quality analysis of TSK n.n. model no. 9 based on random values (recall dataset 3)	72
Figure 4-17: Comparison of TSK n.n. model no. 9 output for recall data and original states used for generation of the data	72
Figure 4-18: Quality analysis of TSK n. model no. 9 based on random values (recall dataset 3). Both input and output data were denormalized for better illustrativeness	75
Figure 4-19: Comparison of denormalized TSK n. model no. 9 outputs for recall data and original states used for generation of the data	75
Figure 4-20: Comparison of outputs of the best-choice models for the recall dataset no. 3 (after subtraction of original states)	77
Figure 5-1: Comparison of original states used for data generation (red), output of FM models (black), output of FM model with zero input no. 2 (blue), and output of FM model with zero input no. 13 (green). The black and green lines overlap perfectly until input vector no. 210	81
Figure 5-2: Sensitivity analysis of MLP model no. 7: original states used for data generation (red), original MLP model output (black), output of MLP model with zero input no. 7, and the difference between these two outputs (green)	82
Figure 5-3: Sensitivity analysis of MLP model no. 7: original states used for data generation (red), original model output (black), output of the model with zero input no. 2, and the difference between these two outputs (green)	82

Figure 5-4:	Sensitivity analysis of TSK n.n. model no. 9: original states used for data generation (red), original model output (black), output of the model with zero input no. 3, and the difference between these two outputs (green)	84
Figure 5-5:	Sensitivity analysis graph of FM model – random failure of input no. 8: original states used for data generation (red), original model output (black), output of the model with random input no. 8, and the difference between these two outputs (green)	86
Figure 5-6:	Sensitivity analysis graph of FM model – random failure of inputs no. 8 and 9: original states used for data generation (red), original model output (black), output of the model with random inputs no. 8 and 9, and the difference between these two outputs (green)	87
Figure 5-7:	Sensitivity analysis graph of MLP model no. 12 – random failure of input no. 13: original states used for data generation (red), original model output (black), output of the model with random input no. 13, and the difference between these two outputs (green)	88
Figure 5-8:	Sensitivity analysis graph of TSK n. model no. 9 – random failure of inputs no. 4 and 5: original states used for data generation (red), original model output (black), output of the model with random inputs no. 4 and 5, and the difference between these two outputs (green).....	89

List of Tables

Table 4-1:	Training data for development of models (part 1/2).....	51
Table 4-2:	Training data for development of models (part 2/2).....	52
Table 4-3:	Correlation factors of generated training data	53
Table 4-4:	Example of test dataset creation – interpolation between state 0 and state 1	54
Table 4-5:	Evaluation of FM model based on training data.....	58
Table 4-6:	Evaluation of FM model based on test data.....	59
Table 4-7:	Overview of architectures of all trained MLPs and their respective errors ...	63
Table 4-8:	Statistical properties of weights of the MLP models.....	64
Table 4-9:	Correlation weights of MLP models compared with empirical correlation factors of input data (part 1/3)	65
Table 4-10:	Correlation weights of MLP models compared with empirical correlation factors of input data (part 2/3)	65
Table 4-11:	Correlation weights of MLP models compared with empirical correlation factors of the input data (part 3/3)	66
Table 4-12:	Overview of TSK models trained using not normalized data and their respective errors	70
Table 4-13:	Outputs of TSK n.n. models for test input vectors and their comparison with desired outputs. The outputs whose errors exceed allowed bounds are marked red	70
Table 4-14:	Comparison of correlation coefficients of TSK n.n. models with empirical correlation factors	71
Table 4-15:	Overview of TSK models trained using normalized data and their respective errors (after denormalization)	73
Table 4-16:	Rescaled outputs of TSK n. models for test input vectors and their comparison with desired outputs. The outputs whose errors exceed allowed bounds are marked red	73
Table 4-17:	Comparison of correlation coefficients of TSK n. models with empirical correlation factors	74
Table 5-1:	Range of random values used for data generation in sensitivity analysis	78
Table 5-2:	Sums of differences of model outputs caused by zero failure of single inputs (maximum values marked red, minimum values marked green).....	79

Table 5-3:	Sums of differences of model outputs caused by zero failure of two adjacent inputs (maximum values marked red, minimum values marked green).....	80
Table 5-4:	Sums of differences of model outputs caused by random failure of single inputs (maximum values marked red, minimum values marked green).....	85
Table 5-5:	Sums of differences of model outputs caused by random failure of two adjacent inputs (maximum values marked red, minimum values marked green).....	85
Table A-1:	Training data for development of models – numbers of states as used for training of the models (part 1/2)	96
Table A-2:	Training data for development of models – numbers of states as used for training of the models (part 2/2)	96
Table B-1:	Test data for development of the models – numbers of states as used for development of the models (part 1/2)	97
Table B-2:	Test data for development of the models – numbers of states as used for development of the models (part 2/2)	97

List of Abbreviations and Symbols

Abbreviation	Description
ADOM	Aggregate degree of membership
ANN	Artificial neural network
BWR	Boiling water reactor
cl.	cluster
COG	Center of gravity
corr.	correlation
COS	Center of sums
err.	error
FM	Fuzzy model by Mamdani
FOM	First of maxima
HL	Hidden layer
lin.	linear (TF)
LOCA	Loss-of-coolant accident
LOM	Last of maxima
LOOP	Loss of off-site power
LWR	Light water reactor
MF	Membership function
MLP	Multilayer perceptron
MOM	Mean of maxima
NPP	Nuclear power plant
PWR	Pressurized water reactor
RPV	Reactor pressure vessel
SC(M)	Soft computing (method/model)
sigm.	sigmoidal (TF)
SOM	Self-organizing map
tanh	hyperbolic tangent (TF)
te.	test
TF/AF	Transfer function / Activation function
tr./train.	training
TSK	Fuzzy model by Takagi-Sugeno-Kang
TSK n.	TSK model trained by use of normalized data
TSK n.n.	TSK model trained by use of not normalized data

WNA	World Nuclear Association
Symbol	Description
A	property of linguistic input variable in fuzzy rules (FM) / membership function (TSK)
B_{in}	property of linguistic output variable in fuzzy rules
b_{0c_m}	bias value of cluster c_m
$b_{x_n c_m}$	coeff. of linear relationship in TSK systems
β	bias of neuron (MLP)
c_i	cluster center
δ	width of Gaussian function (TSK) / difference between target and model output (MLP)
$ E $	absolute square error
$ e $	relative square error
$ \bar{E} $	absolute mean square error
$ \bar{e} $	relative mean square error
f	activation function
g_{ci}	normalized membership degree
G_{ij}	elements of matrix of weight factors
K_{xy}	TSK-correlation coefficients
m	number of clusters
n	number of inputs
η	coefficient of learning rate
R_i	fuzzy rule
r/r_{xy}	correlation factor
σ	width of Gaussian function
u_i	fuzzy variable
w	weight of connection (MLP)
X/x	input variable
Y/y	output variable
Ψ	matrix of correlation weights

1 Introduction

1.1 Position of the work

This master thesis is a part of the project ‘Non-Invasive Condition Monitoring of Nuclear Reactors for Detection of Level Change and Deformation of the Core’ (German: **Nichtinvasive Zustandsüberwachung von Kernreaktoren zur Detektion von Füllstandsänderungen und der Deformation des Kerns - NIZUK**), funded by the German Federal Ministry of Education and Research. The project is held in cooperation between Zittau/Görlitz University of Applied Sciences, Institute of Process Technology, Process Automation and Measuring Technology (IPM) and Dresden Technical University. The task of the project is to develop a measuring system for diagnosis of core state of LWR.

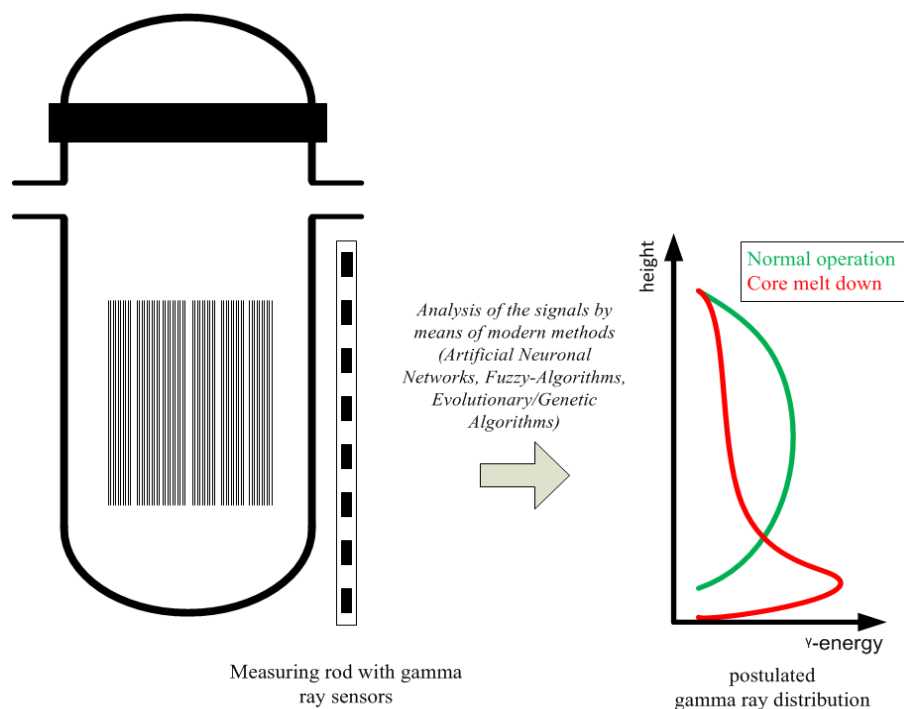


Figure 1-1: Schematic principle of measurement for detection of core meltdown (side view of RPV)

The principle of the measurements is to be based on gamma ray distribution measurement outside of the reactor pressure vessel (figure 1-1). Gamma ray sensors are to be arranged in one or more vertical measuring rods reaching from upper edge of the core to the lower plenum of the reactor vessel. The basic idea behind the measurements is that the core materials as well as the radioactive fission product relocate during a core meltdown process. This causes a continuous change of the gamma distribution outside the RPV which can be measured and the change of state detected.

The outputs of the gamma sensors are to be analyzed using modern methods (soft computing – fuzzy algorithms, artificial neural networks, etc.). Creation of such models and their subsequent analysis in terms of dynamics and sensitivity are the aim of this thesis.

1.2 Objective of the work

The main objective of the thesis is to create soft computing models for core state detection. The motivation for the work is to ascertain a suitability of selected SCMs for use in this particular project, i.e. classification of core states during a core meltdown.

Firstly, datasets for development and quality analysis of the models are to be generated based on postulated gamma distribution outside the RPV during individual core states of a nuclear meltdown [1]. Next, suitable Soft Computing Methods and associated appropriate simulation tools are to be chosen. Requirements for models quality are to be stated and methods of its assessment described. The SC models are to be developed and their quality evaluated based on this theoretical knowledge.

Sensitivity analysis of all developed models is to be performed next. Behavior of the models is to be analyzed in cases of various failures of their inputs – gamma ray sensors. The results will be compared and measures to minimize the effects of the failures suggested.

1.3 Structure of the work

Theoretical basics of the thesis are stated in chapter 2. Since the project is conducted with aim on increasing safety of nuclear power plants, namely pressurized water reactor power plants, basic knowledge regarding functionality and radioactive inventory of the PWR, fission products and a possible choice for gamma ray sensor is provided at the beginning of the chapter. The phenomenon of core meltdown is introduced next and individual phases of the event are described. As the last, and the most extensive, part of the ‘state of the art’ chapter, the soft computing methods are presented. The work is focused on three types of SC models – MLP, and fuzzy models by Mamdani and by Takagi-Sugeno-Kang.

Chapter no. 3 is dedicated to methods of model quality analysis. Three methods are described: error based methods where standard types of errors are defined, internal parameters based

methods – two techniques used for multilayer perceptrons and one method for TSK-models, and random values based method, applicable for all selected types of models.

At the beginning of chapter 4, general method for development is introduced in detail, followed by the description of all datasets generated for development and quality analysis of the models. The error limits and other criteria which the models must satisfy are stated in section 4.2. The rest of the chapter is dedicated to detailed description of development and subsequent quality analyses of SC models. The models are compared in terms of their error characteristics and quality analysis based on random numbers at the end of the chapter.

The general method for sensibility analysis with description of assumed input failures and generation of input datasets is introduced at the beginning of chapter 5. Results of both assumed input failure for the three types of models are reviewed next. At the end, the summary of sensitivity analysis and following suggestions to improve the behavior of the models in case of input failure are given.

2 General Basics

2.1 Pressurized Water Reactors

Most of the nuclear reactors worldwide are used for commercial electricity generation. The design of such reactors is continuously subject of development as the technological possibilities grow. The first generation of them is usually referred to as ‘Early Prototype Reactors’, activated in late 1950’s and 1960’s in the USA (Shippingport, Dresden, Fermi 1) or UK (Magnox) [2].

Present-day statistical publications state that the majority of currently operating commercial reactors is of Generation II – Light Water Reactors (LWR). Although some other principles besides LWR were presented in the Generation II, such as Advanced Gas-cooled Reactor (AGR) used in the UK, Russian Light-Water-cooled Graphite-moderated Reactor (RBMK), or Canadian CANDU reactor, the Light Water Reactors, namely Pressurized Water Reactors constitute absolute majority of all western nuclear power plants.

According to World Nuclear Association (WNA), 60 % of worldwide reactors are PWRs. In Germany, there are currently 7 operational PWRs listed in WNA Reactor Database [3] with total net capacity of 9.5 GW and 4 more were shut down since 2010. As for Boiling Water Reactors (BWRs), the worldwide share is ca. 21 % and there are 2 operational reactors in Germany after 4 others were shut down in last three years.

2.1.1 Design and Functionality

Light Water Reactors make use of light water as both coolant and neutron moderator within the reactor. In PWR (figure 2-1Figure 2-1), pressurized light water is circulated by high-pressure pumps through the core where energy generated by nuclear fission chain reaction is transferred from nuclear fuel rods to the coolant. The heated primary coolant then further transfers the energy to secondary system where steam is produced which is subsequently used for feeding a turbine that spins an electric generator. The exact values of temperature and pressure of primary and secondary systems differ for individual reactor designs but in average the temperature of primary coolant varies from ca. 290 °C as it enters the reactor vessel till approx. 330 °C before it is cooled by the secondary system. The pressure of primary coolant is approx. 15–16 MPa. The temperature of secondary systems ranges between 225 and 285 °C and the pressure is about 6–7 MPa [2].

The fuel elements are located in the core. The enrichment level of uranium varies; the most enriched elements are located in the outer parts of the core, elements with lower level of enrichment are placed in the central region of the core. The nuclear fuel (uranium dioxide, UO_2) is manufactured by pressing and sintering of UO_2 powder into small (height and diameter of ca. 10 mm) and dense (ca. 6 g/cm^3) pellets [4]. The pellets are placed into cladding made of Zircaloy to form a fuel rod with length of ca. 4 meters. Core of a 1300MW reactor by Kraftwerk-Union has 193 fuel elements, each element containing 236 fuel rods, resulting in total uranium mass of 125 t [2].

Reactor pressure vessel with diameter of ca. 5 m and height ca. 13 m surrounds the core. It is designed to cope with the high pressures and temperatures stated above. Besides the fuel elements, it also contains control and safety systems as well as instruments for core monitoring. The RPV, steam generator, high-pressure pumps and other components of NPP are enclosed in the containment. The pressure inside the inner (steel) containment is kept lower than the atmospheric pressure, so that in case of rupture, only leakage from the outside is possible [2]. The outer containment is made of reinforced concrete and is designed to withstand outer impacts, such as airplane crashes or natural disasters.

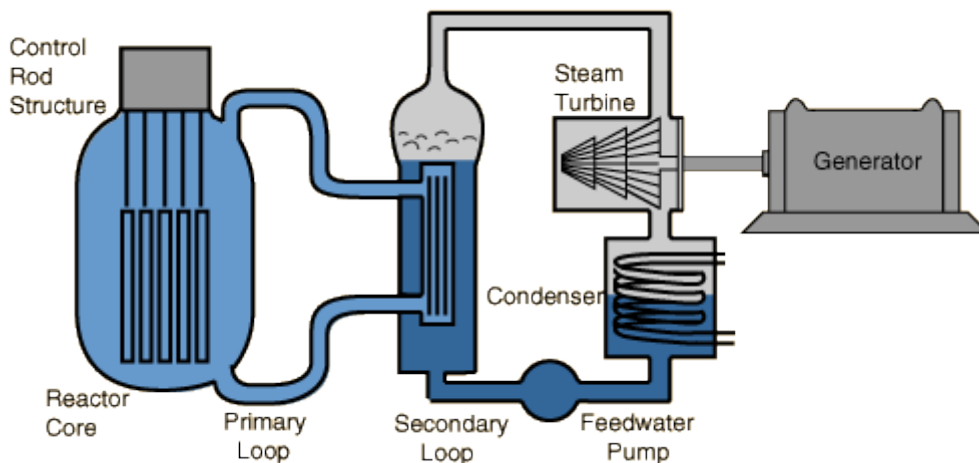


Figure 2-1: Schema of Pressurized Water Reactor (PWR) [5]

2.1.2 Safety Systems

Protection system of a PWR makes use of measurements of data important for the safety of the NPP. It consists of procedures, launched automatically after defined set points are reached.

Reactor trip (scram) is a fast, emergency shutdown of a reactor. During normal operation, neutron-absorbing rods are held above the core by electric motors. In case of emergency, the rods are dropped into the core by gravity (sometimes reinforced by a strong spring). The insertion of the rods stops the nuclear chain reaction. At the same time, emergency cooling system is activated to remove the afterheat (heat produced by natural decay of fission products), or (in cases of loss-of-coolant accidents) to supply for the coolant and prevent the core meltdown.

For cases of public electrical grid breakdown, the NPPs are equipped by emergency power supply. If a blackout occurs, the plant is disconnected from the grid and produces energy only to supply for its requirements. If, however, this isolated operation mode fails, the control and safety systems are to be fed from diesel generators and battery systems.

The emergency feedwater system is one of the systems supplied by the emergency power supply. It is initiated by a decrease of reactor cooling system pressure and substitutes the primary cooling system water in the afterheat removal.

The safety systems (esp. diesel generators and emergency feedwater system) are equipped with high level of redundancy so that the probability of their unavailability in case of emergency is minimized.

2.1.3 Radioactive Inventory in the Reactor Coolant System

Radioactive inventory of a NPP is constituted mainly by fission products. Normally they are contained by the cladding of fuel rods but when a small leak in the cladding appears, the gaseous fission products (esp. noble gasses – krypton and xenon, and tritium) may get into the coolant [2]. Through the coolant purification system and the exhaust air system, they may be released into the environment.

The release of isotopes with shorter half-lives is effectively reduced by their holdup in storage and decay tanks [2]. Most of the tritium (more than 99.9 %) is bound by the zircaloy cladding

and the oxide layer on its surface. When the cladding gets damaged, the tritium contaminates the coolant water.

Besides the three aforementioned isotopes, the fission products consist, in general, of all the elements from zinc to lanthanides [6]. The majority of them is, however, concentrated in two areas (of atomic numbers) – between strontium (38) and ruthenium (44), and from tellurium (52) to neodymium (60). Regarding their chemical properties, the fission products are divided into three classes in terms of their volatility: highly volatile (Xe, Kr, I, Br, Cs, Rb, Se, Te,...), semi-volatile (Ba, Ru, Sr, La, Eu, Ce, Mo) and low-volatile isotopes (Rh, Pd, Tc, Nb, Zr, Tm, Cm, Sm, U, Zn,...) [7].

2.1.4 Barriers of Fission Products

The main task of nuclear safety systems is to prevent the release of radioactive materials into the environment. Four-level system of barriers preventing the release of fission products is applied, consisting of [8]:

- nuclear fuel matrix,
- fuel cladding,
- reactor pressure vessel, and
- containment.

The fuel matrix is the first barrier preventing release of the fission products. The quality of the matrix is largely determined by the manufacturing process. The matrix itself is, however, rather peripheral means of fission products release prevention.

The second and, during the normal operation, the most important fission products barrier is the fuel cladding. Monitoring of the claddings for leakages on regular basis is thus required from the safety point of view. The general monitoring method is based on concentration measurements of certain fission products in the primary coolant system. Concentration monitoring of isotopes with short half-lives may provide several important characteristics, such as type of defect (tight or open) or number of leaking elements, whereas specifications of the leaking element (burn-up or original enrichment of uranium) are observed from long-lived isotopes measurements.

A lot of the research works in last decades regarding safety of the third barrier (RPV) focused on problem of embrittlement. The embrittlement of RPV is a process which directly jeopardizes

the safety of NPP. Especially in the regions of RPV that are close to the core, the neutron radiation considerably rises the brittle-to-ductile temperature, lowering the strength of RPV material and resulting in higher possibility of its fracture. Predicting and resolving such problems have been a subject for a significant number of projects [8].

The containment, as mentioned above, consists of two parts – the inner, gastight steel containment, and the outer shell of steel-reinforced concrete. While the inner part is designed to withhold any releases of the radioactive material, the outer containment serves mostly as a protection from the external impacts, and its up to 2 meters thick walls also absorb the gamma radiation.

2.2 Core Meltdown in PWR

Nuclear meltdown is a result of series of events starting by phenomena stated in sect. 2.2.1, and ending with partial or total melting of the core material, the latter leading to molten material relocation into lower plenum of reactor vessel. There have been several projects studying core degradation ([9], [10]). Analysis of TMI-2 accident ([11], [12]) is an important and frequent source of knowledge. In general, a core meltdown in PWR is triggered by an insufficient heat removal from the reactor core over a longer time period.

There are several ways of dividing the individual phases of core meltdown. The basic division is the In-vessel vs. Ex-vessel phase. The in-vessel phase is in general better understood, due to a large number of research projects and the TMI-2 accident analyses. It is further separated into 2–4 phases. Most studies introduce so called ‘early’ and ‘late’ in-vessel phase. The early in-vessel phase is characterized by melting of metallic materials. Cooling system failure leads to overheat of the core and the fuel rod’s cladding, the control rods, Inconel grid spacer and/or other elements start to melt. The most significant phenomenon of the late in-vessel is melting of ceramic materials and loss of rod-like geometry of core elements.

With respect to the focus of this project, only the in-vessel phase is taken into account in this document.

2.2.1 Initiating events

There are two main scenarios of events preceding the nuclear meltdown [13]:

- loss of off-site power (LOOP) and
- loss of coolant accidents (LOCA).

The LOOP scenario (also referred to as high-pressure scenario) is connected with complete failure of the power supply (station blackout). The diesel generators are also assumed to be unavailable in this scenario. Reactor safety systems as well as valves may be operated using battery power for a limited time but the core reflooding which would prevent the severe accident cannot be performed due to unavailability of pumps. In normal operation, the loss of off-site power would cause the emergency shutdown of the reactor (reactor trip) and decay heat would be removed by the diesel generator powered pumps [14].

The low-pressure scenario (LOCA) is initiated by a rupture of a cooling system pipe. The loss of coolant results in significant temperature escalation as there is not enough capacity to remove the heat produced by fission reactions. In combination with a safety system failure, this ultimately leads to a core meltdown.

2.2.2 Early In-Vessel Phase

Series of events starting with initial fuel cladding degradation and leading to melting and relocation of the metallic materials of the core is referred to as the early in-vessel phase. This particular phase is a well-understood phase of the core meltdown due to number of experiments regarding this phenomenon (PBF-SFD, PHEBUS-SFD, CORA and more) [9].

The early phase of the core degradation is triggered by a decrease of coolant water level. The heat from the core thus is not sufficiently removed, leading to temperature escalation. Once ca. 30 % of the core is exposed (not surrounded by coolant) the degradation of some core materials occurs.

As the temperature rises, the pressurized water (liquid under normal operation conditions) boils. The incident water steam then penetrates into the containment, either through the primary cooling system leakage (LOCA) or via the supply valves (LOOP). Once the temperature exceeds ca. 730 °C, the zircaloy cladding of the fuel rods begins to oxidize in incident flow of steam resulting in hydrogen production and creation of an oxide layer on the claddings. In

addition, the oxidation, being an exothermic reaction, increases the temperature inside the reactor vessel which further raises the oxidation rate, leading to uncontrolled temperature escalation. A significant increase (up to 10-20fold) of the temperature rise rate occurs above 1300-1400 °C.

The control rods are the first components to melt and relocate into lower regions of the reactor vessel. As the oxidation goes on (at ca. 1700-1800 °C), the oxide layer becomes thick enough that it is capable to retain the metallic material which would melt inside. Once these molten materials penetrate the oxide shell, the heatup rate of fuel material falls down promptly. Afterwards, the metallic materials flow down to the lower and cooler regions where they may refreeze and create a metallic barrier.

The overall time between the initial safety failure and the final melting of the core may vary from as short as 10 minutes to extensive time periods of 8–10 hours. The progresses of individual meltdowns differ largely depending on initial conditions, reactor type or the duration of triggering events.

Three significant core states during the early phase were defined (figure 2-2Figure 2-2, states 1-1 to 1-3). In state 1-1, a leakage in the cooling system causes loss of coolant, resulting in partial core exposure with a possibility of fuel cladding degradation. The metallic material begins to melt (state 1-2) and relocates into lower, colder regions (state 1-3) while the ceramic parts preserve their rod-like geometry.

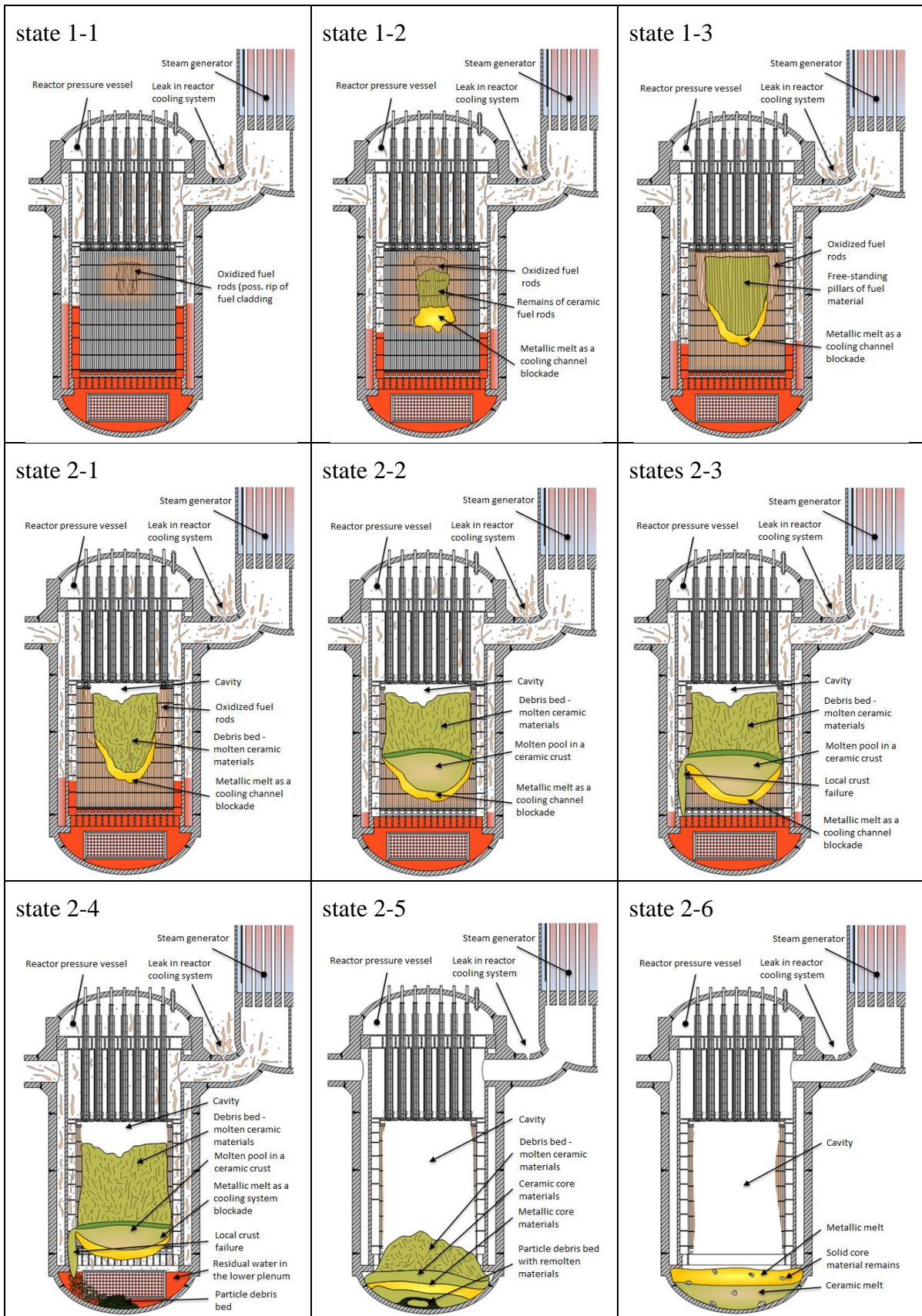


Figure 2-2: Significant core states during core meltdown in LWR [1]

2.2.3 Late In-Vessel Phase

The late in-vessel phase is characterized by the loss of rod-like geometry, the formation of fuel debris region which subsequently evolves into a molten pool whose periphery migrates and the molten core material can be released into the lower plenum. In contrast to the early phase, it is related to melting of ceramic core materials.

The late phase is associated with phenomena such as formations of debris bed, molten pools and cavity on the top of the core. The debris bed consists of fragments of fuel cladding and fuel pellets. There have been several researches about cooling of the debris bed. Although it is necessary to be cooled, the reflooding of the core introduces some significant risks. It leads to massive steam production which increases the pressure inside the RPV. Furthermore, an oxidation of relocated metallic materials may occur, again generating hydrogen which may cause explosive reactions (as at Fukushima).

The ongoing heatup of the debris bed may cause molten pool formation – molten ceramic core material retained by ceramic crust. The molten pool may grow in both axial and radial directions, consuming the crust and reaching the boundaries of the core [12]. Ultimately, it may lead to crust failure and large core melt relocation into the lower plenum of the RPV. How much of the core material would relocate and when the relocation would occur depend on several factors including:

- crust failure size and location,
- the total mass of nuclear fuel, fission products, control rods and other elements of the core (corium),
- the composition and temperature of the corium,
- states of core structures,
- surface chemical interactions, and
- processes of crust formation.

A total of six significant states were defined for the late in-vessel phase (see figure 2-2Figure 2-2, states 2-1 to 2-6). Formation of a cavity and debris bed – loss of rod-like geometry – is depicted in state 2-1. State 2-2- shows formation of a molten pool contained by a ceramic crust. In state 2-3, a local crust failure occurs and molten ceramic material is released, resulting in formation of particle debris bed in the lower plenum (state 2-4). Residual water is evaporated and all the material relocated in state 2-5. The end-state configuration of a core meltdown in a LWR is represented by state 2-6.

2.2.4 Gamma distribution for the low-pressure scenario

Based on significant states depicted on figure 2-2, distribution of gamma radiation outside the RPV during a core meltdown was postulated [1]. Following phenomena were taken into account while producing the gamma distributions:

- loss of coolant – lower absorbance of gamma radiation,
- formation of cavity,
- relocation of radioactive material, etc.

In figure 2-3, postulated distribution of gamma radiation outside the RPV during a core meltdown is depicted, based on defined significant core states (figure 2-2). The expected distribution during a normal operation is marked green, the distribution for individual states red.

In the first three states, representing the early in-vessel phase, a loss of coolant and subsequent melting and relocation of metallic materials are taken into account. The absence of these substances and associated lower absorbance of the gamma radiation results in higher activity in the upper parts of the core as seen in states 1-1, 1-2 and 1-3 (figure 2-3).

The formation of cavity causes rapid decrease of the activity in the upper core region at the beginning of the late in-vessel phase (state 2-1). The creation of the molten pool (state 2-2) causes a higher concentration of radioactive materials in the mid-core region, leading to a peak in the gamma distribution. The crust failure (state 2-3) and a release of radioactive materials formerly contained within the molten pool lead to a higher activity in the lower part of the core. As the molten material relocates into the lower plenum (state 2-4), the first activity is recorded beneath the core. Simultaneously, the cavity in the upper regions grows, resulting in larger area with low activity and ultimately leading to relocation of all core material into the lower plenum (state 2-5). The segregation of metallic and ceramic melt (state 2-6) causes the steps in the distribution function.

The gamma distribution, resp. the radioactive activity along the height of the core and lower plenum is expected to be measured by means of gamma ray spectrometers. It was mentioned before that the core states are to be diagnosed based on relocation of radioactive materials and the associated change of gamma distribution outside the RPV. In that regard, monitoring the movement of all fission products may be redundant and less accurate than measurement focused on a narrow spectrum of isotopes.

One of suitable possibilities of measurement is a use of scintillation counters as they can measure the activity in dependence on gamma energy, and since each isotope can be detected based on its specific frequency of gamma radiation, the movement only of some selected (non-volatile) fission products can be monitored.

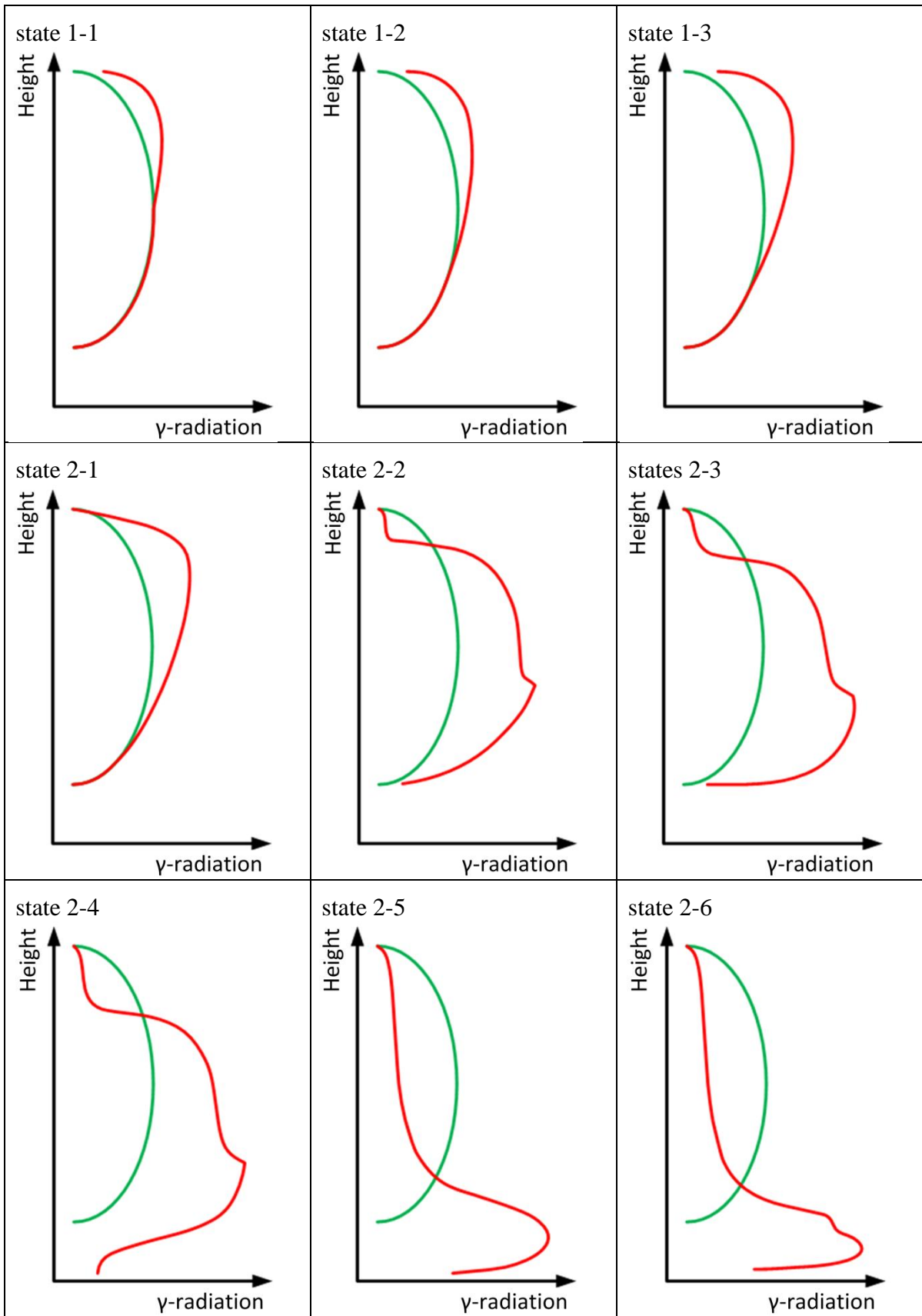


Figure 2-3: Postulated gamma distribution based on core states from figure 2-2 **Figure 2-2 [1]**

2.3 Soft Computing Methods

A lot of real world problems may be solved using the Soft Computing Methods (SCMs). They become more and more popular ever since early 1990's. Rather simple problems could be analyzed by early SCM approaches. The current state of development makes it possible that they can be used for complicated and complex systems' analyses not only in technical sciences but also in biology, medicine, and human or management sciences.

The list of the most commonly used SC methods includes:

- Fuzzy Logics,
- Artificial Neural Networks, or
- Genetic Algorithms.

Mutual characteristic of all these methods is their tolerance of uncertainties. Unlike the standard, hard computing methods which search for an exact solution, the SCMs approximate the system with certain level of imprecision.

2.3.1 Fuzzy Systems by Mamdani

The basic idea behind fuzzy logic is to unify physical world (described by numerical expressions) and human world (working with linguistic expressions). It was introduced for the first time in 1965 by L. A. Zadeh [15]. A fuzzy set is there described as a class of objects with continuum of grades of membership. Standard logic makes use of binary sets. The value of such variables is either 0 (false), or 1 (true). The truth value of fuzzy sets, in contrast, ranges in the whole interval between 0 and 1.

2.3.1.1 Membership functions

The degree of membership of a variable into a binary (crisp) set is characterized by a rectangle of height 1 and width defined by boundary values of the set. In fuzzy theory, there are more possibilities to define such membership function (MF). The most common choices are (see figure 2-4Figure 2-4):

- triangular function (a),
- trapezoidal function (b),
- Gaussian function (c),

- generalized bell function (d),
- Π -shaped function (e),
- sigmoidal function (f), or
- S- and Z-shaped functions (g and h)

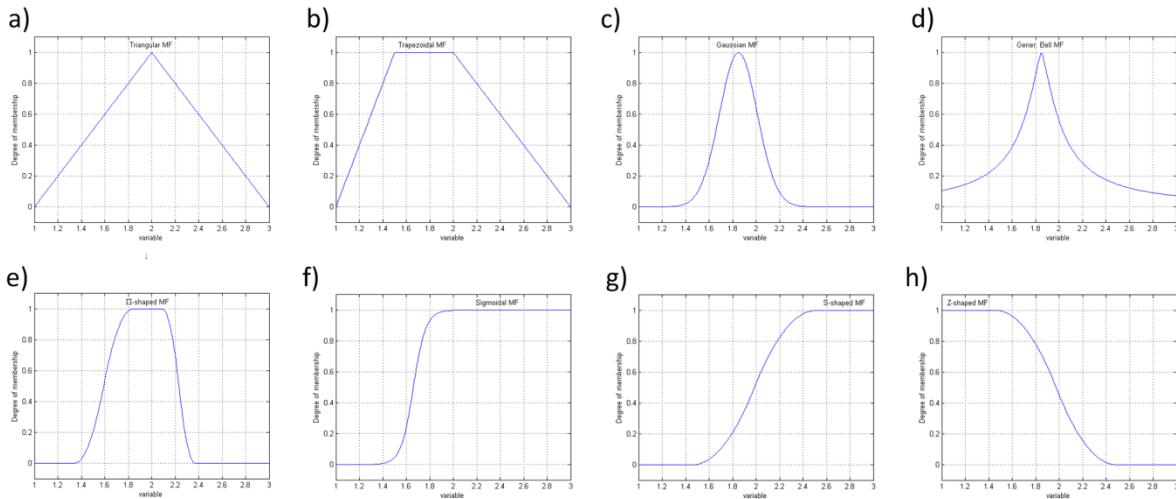


Figure 2-4: Standard membership functions

2.3.1.2 Fuzzy rules

The standard way to describe a system by fuzzy model is by a set of fuzzy rules. The rules are in the form of IF-THEN, typically: If *variable1* is *property of var1*, and (or) *variable2* is *property of var2*, and (or) ... then *output* is *property of output*. Common notation of set of fuzzy rules:

$$R_i: \text{IF } X_1 \text{ is } A_{i1} \text{ AND } \dots \text{ AND } X_n \text{ is } A_{in} \text{ THEN } Y \text{ is } B_i \quad (2-1)$$

Properties are described by membership functions as shown on figure 2-5. The part of the rule after IF and before THEN is called antecedent or premise; the part after THEN is called succedent or conclusion.

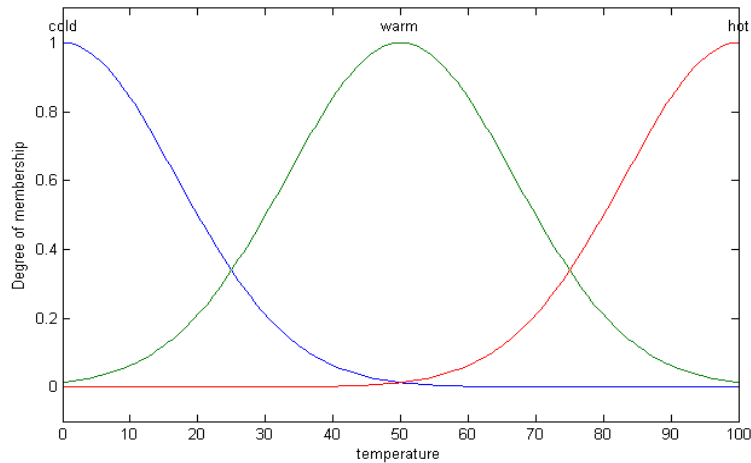


Figure 2-5: Typical arrangement of membership functions of a fuzzy variable

In case variable1 was temperature of water, one would be able to distinguish between three states: cold, warm and hot, but with no strict boundaries. The water is absolutely cold only at 0 °C. As the temperature rises, the water is still cold but with lower degree of membership. It also becomes somehow warm, although the membership degree is very low. At about 25 °C, the water is cold and warm with the same degree of membership at the same time. With further temperature rise, it becomes less and less cold and more and more warm.

The process of transforming sharp, real-world value into grades of membership for linguistic terms of a fuzzy set is called *fuzzification*. Such definition of variables is much closer to human thinking than the binary statement: Water is absolutely cold between 0 and 25 °C, after that it instantly stops being cold and is warm.

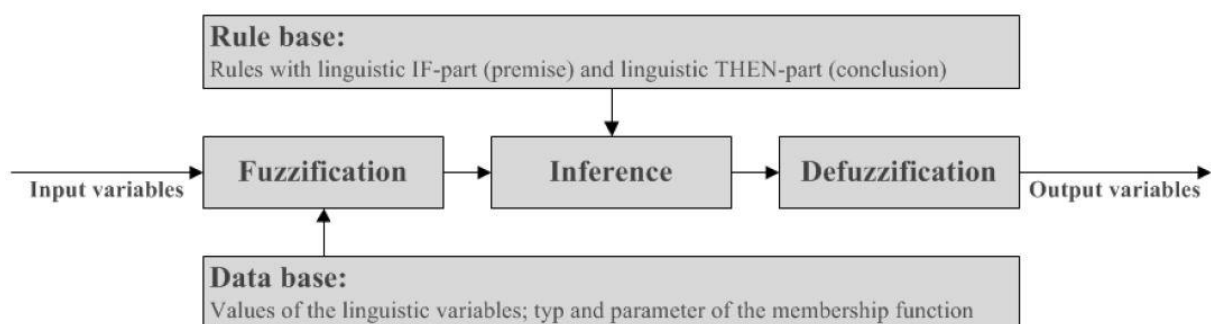


Figure 2-6: Schema of a fuzzy system by Mamdani [16]

Figure 2-6 shows components and schema of a Mamdani fuzzy model. After a crisp input variable is fuzzified with use of data base containing linguistic variables with appropriate membership functions, it infers which means that all rules from the rule based are evaluated

and a result fuzzy set is produced based on linguistic output variables and strength of corresponding rules.

The inference consists of three parts: (1) premise evaluation – determination of aggregate degree of membership, strength of the rule, (2) rule activation (implementation) – application of the strength of the rule to its respective output membership function, and (3) aggregation – combination of rules with nonzero strength.

2.3.1.3 Methods of operators

In order to transform the linguistic rules into fuzzy sets, methods for operations (namely: AND, OR, Implication, Aggregation of Defuzzification) must be defined.

The AND and OR methods determine, how expressions in antecedent are combined. The most common method for AND operator is *minimum*, meaning the lowest degree of membership of the inputs for each rule will be the aggregate membership degree of the whole antecedent. Another possibility, regularly used, is *product*. By analogy, the most common method for OR is *maximum*. Alternatively *probabilistic OR* (also known as the *algebraic sum*) may be used. It is defined as:

$$probor(a, b) = a + b - ab \quad (2-2)$$

The implementation method then defines how the aggregate degree of membership (ADOM) of antecedent reshapes the membership function of respective output variable. The common choice is the same as by AND: *minimum* or *product*. When applying the minimum method, the shape of the output MF beneath the antecedent ADOM remains the same and is bounded from above by this value. The product method simply multiplies the output MF by the ADOM.

The aggregation methods (not to be related with the aggregate degree of membership) are responsible for creation of a fuzzy set resulting from combination of all the rules. Fuzzy sets of each rule are characterized by the membership function of the output after application of implementation method. The prevalent method is the *maximum* function. Other possibility is, as by the OR methods, *probabilistic OR*. The last commonly used method of aggregation is *summation*.

The defuzzification method determines how actual output value will be read from the resulting fuzzy set from previous paragraph. *Center of Gravity* (COG) method is the most natural and

the most frequently used defuzzification method. The output value is calculated as geometrical center of area of the resulting fuzzy set:

$$COG(A) = \frac{\sum_{i=1}^n A(u_i) \cdot u_i}{\sum_{i=1}^n A(u_i)}, \quad (2-3)$$

where n is number of membership functions of respective output, $A(u_i)$ is degree of membership of fuzzy variable u_i into the resulting fuzzy set.

Defuzzification using *Mean of Maxima* (MOM) method is also often used, especially when lower computation effort is required. Other defuzzification methods are rather peripheral and include *First of Maxima* (FOM), *Last of Maxima* (LOM) or *Center of Sums* (COS).

2.3.1.4 Example – ‘Tipper’

For better illustration, a rule diagram of classical fuzzy example ‘Tipper’ is provided below. The system has two inputs: quality of service with three MFs (poor, good and excellent) and quality of food (rancid or delicious with blank space in between), one output, the tip (cheap, average or generous), and three rules: (1) If *service* is *poor* or *food* is *rancid* then *tip* is *cheap*, (2) if *service* is *good* then *tip* is *average*, and (3) if *service* is *excellent* or *food* is *delicious* then *tip* is *generous*. The methods were chosen:

AND method:	<i>minimum</i>
OR method:	<i>maximum</i>
Implication:	<i>product</i>
Aggregation:	<i>maximum</i>
Defuzzification:	<i>COG</i>

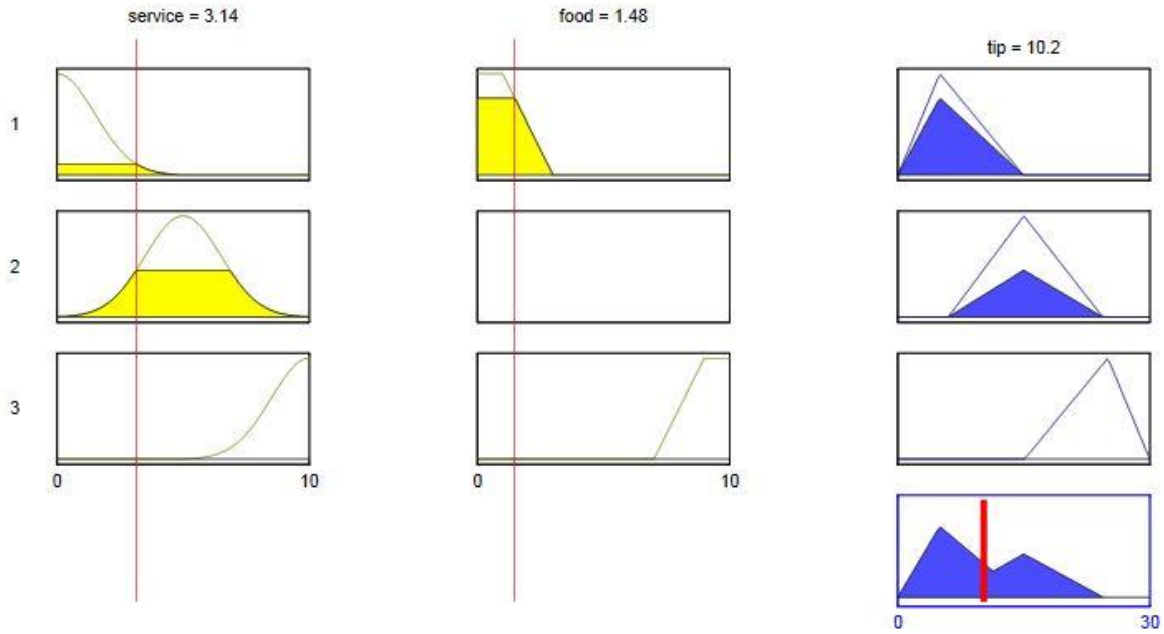


Figure 2-7: Rule diagram of example system ‘Tipper’

2.3.2 Fuzzy Systems by Takagi-Sugeno-Kang

The Mamdani model of fuzzy systems is referred to as relational fuzzy system. In contrast, the Takagi-Sugeno-Kang model (TSK) is called *functional* system. Several features are common for these two models; such as the process of fuzzification (transformation of crisp numeric values into degree of membership of a linguistic value), structure of data base (linguistic variables, type and parameters of membership functions) or evaluation of the first, IF- part of the fuzzy rules (calculation of aggregate degree of membership of antecedent).

The TSK models differ from Mamdani in a number of aspects. General definition of TSK-systems is also by the set of fuzzy rules with the same premise as by Mamdani but with different (functional) conclusion:

$$R_i: \text{IF } X_1 \text{ is } A_{i1} \text{ AND } \dots \text{ AND } X_n \text{ is } A_{in} \text{ THEN } Y_i = f_i(X_1, \dots, X_n) \quad (2-4)$$

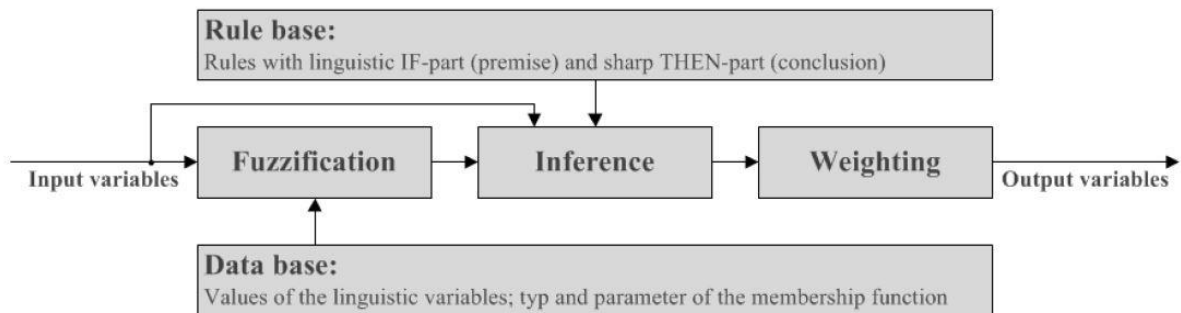


Figure 2-8: Schema of a fuzzy system by Takagi-Sugeno-Kang [16]

The premise evaluation is done the same way as by Mamdani but the rule activation is done by calculation of a sharp value of the output function of each rule which is then multiplied by the degree of fulfillment. The last part of inference – the aggregation – is performed by superposition of the values acquired from rule activation.

Weighting process is used as an alternative to Mamdani’s defuzzification. The sharp value of output variable is determined by a weighted average of the sharp output values of the rules.

The TSK models are of great applicability in cases when it is known that the original system of which a model shall be created is non-linear, however it may be partially linearized even if the areas or linearity cannot be pinpointed. The TSK rules are hard to establish by experience. They are usually generated using datasets.

2.3.2.1 TSK-Systems with the Cluster Algorithm by Wong and Chen

For use in this project, a special type of TSK model is suitable. It makes use of a clustering-based method for fuzzy modeling [17].

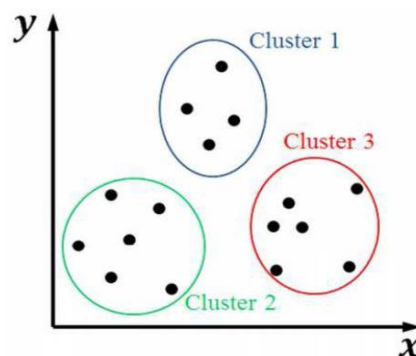


Figure 2-9: Division of dataset with input and output data into clusters [18]

Similarly to MLP model (see sect. 2.3.3), the design of TSK-model with the cluster algorithm by Wong and Chen is conducted by a process of training. The training takes place in two steps: (1) Structure identification, and (2) Parameter identification.

In the first step, the data of the input and output variables are analyzed using the aforementioned clustering algorithm. The structure of the model is characterized by number of clusters m and centers of the clusters c_1, c_2, \dots, c_m . Both these characteristics can be affected by parameter σ and determine a degree of freedom of the TSK-model by Wong and Chen. Decrease of the parameter σ causes increase of the number of clusters.

After the structure has been identified, the second step – parameter identification – is performed. Its purpose is to ascertain coefficients representing linear relationship between input and output variables $b_{x_n c_m}$ (n is number of inputs) and bias values for each cluster $b_{0_{cm}}$.

The aim of the training is to develop an approximately exact replica of the relationships between input and output variables. The criteria to determine whether the training was or was not successful often include demand of maximum error (difference between real and model output for every data pattern of the training dataset).

As a result of the training, a set of rules R_i ($i = 1, \dots, m$) is established:

$$R_i: IF (x_1 \dots x_n) \text{ is } A_i \text{ THEN } y \text{ is } y_i = b_{0_{ci}} + \sum_{j=1}^n b_{x_j c_i} \cdot x_j \quad (2-5)$$

where A_i is a membership function:

$$A_i = \exp\left(-\frac{\sum_{j=1}^n (x_j - c_i)^2}{2 \cdot (\delta_i)^2}\right) \quad (2-6)$$

where δ_i is the width of the Gaussian function, a proposal for determining appropriate δ_i is provided in [17]. A_i is then used to calculate normalized membership degrees g_{ci} :

$$g_{ci} = \frac{A_i}{\sum_i A_i} \quad (2-7)$$

And the value of the output variable y can be calculated by summarizing all y_i :

$$y = \frac{\sum_i y_i \cdot g_{ci}}{\sum_i g_{ci}} \quad (2-8)$$

The structure of TSK-model of discussed type can be compared with a MLP with one hidden layer. Instead of neurons, it consists of clusters, each with specific bias value. The connections between inputs and clusters describe the linear part of the model, the non-linear relationships between input and output variables is characterized by the connections from clusters to the outputs (see figure 2-10).

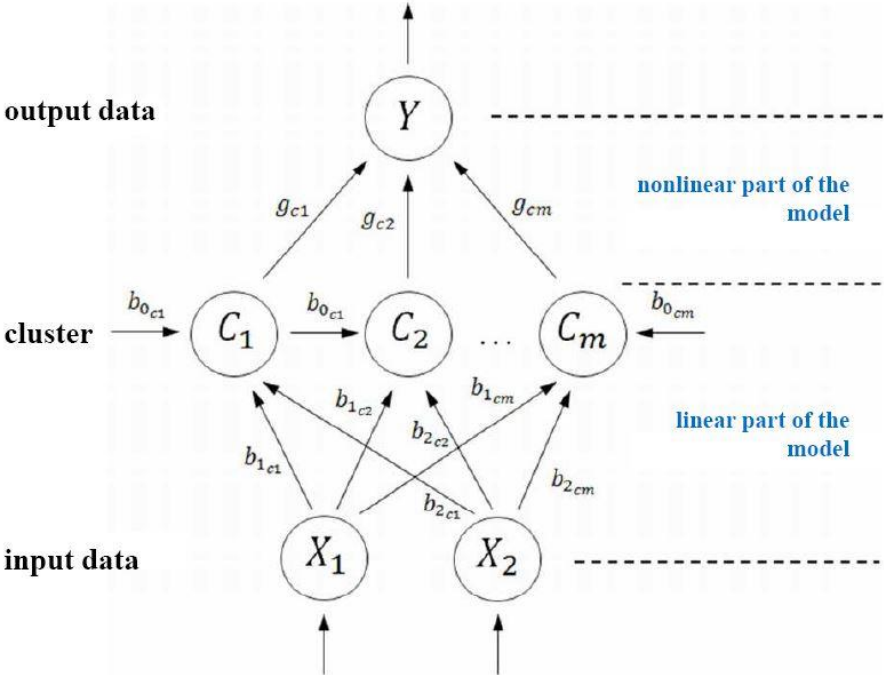


Figure 2-10: Schema of a TSK model with the cluster algorithm by Wong and Chen [18]

The linear part coefficients and the cluster biases are subject of training and do not change after the structure and parameter identification is completed. As follows from equations (2-5) and (2-6), the coefficients of the non-linear part g_1, g_2, \dots, g_m are recalculated for every data pattern.

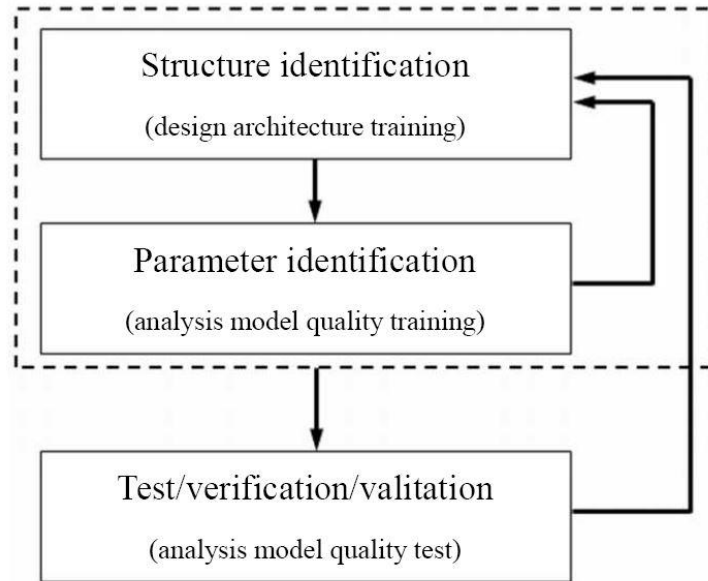


Figure 2-11: Block diagram of design of TSK-model with the cluster algorithm by Wong and Chen [18]

The test and verification of the model is performed following successful training (dotted line surrounded area in figure 2-11). In this last phase of the model design, a dataset which was not involved in the training is used. The purpose of the test is to verify whether the model truly ‘understood’ the real physical system and returns correct outputs for the input data patterns with which it was not trained. The deciding criteria for correctness of the model are also related to maximum allowed error of the model outputs with respect to the real system’s outputs.

2.3.3 Multilayer Perceptrons

Function of human brain served as a role model for development of Artificial Neural Networks (ANN) method. ‘Neurons’, each with specific, rather simple transfer function, when connected into a net, may solve complex, non-linear problems.

There are two main classes of ANNs: Multilayer Perceptron (MLP) and Self-Organizing Map (SOM). The self-organizing maps (sometimes called Kohonen map) make use of so called unsupervised learning and are more suitable for clustering or visualization of high-dimensional data. The MLP, on the other hand, is trained by supervised learning and is used for pattern recognition and modeling of non-linear system. For further work, artificial neural network in form of MLP is considered.

The MLP model is characterized by three kinds of layers: The input layer with one neuron assigned for each input of the real system, the hidden layers (usually one or two) with arbitrary number of neurons, and the output layer, again with one neuron for each output of the real system. The neurons are connected via ‘synapses’. These connections may only link one neuron with another one from neighboring layer. No connections within one layer or between the next but one layers are permitted. Each individual synapse is characterized by a parameter of *weight*. It is a factor which multiplies output of source neuron.

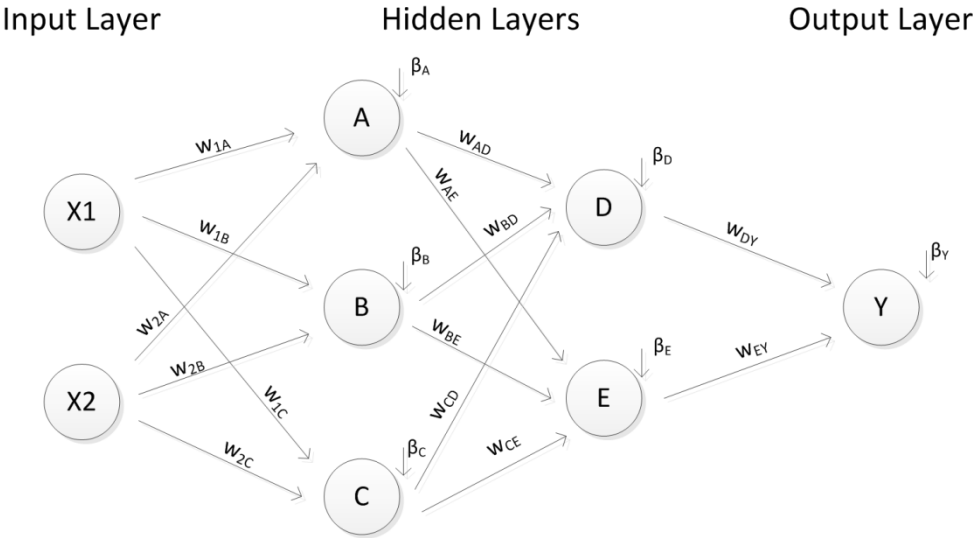


Figure 2-12: General structure of an artificial neural network

The real system described by the model depicted on figure 2-12 has two inputs, thus two neurons in input layer, X1 and X2. The model has two hidden layers, the first one with three neutrons (A, B, and C), and the second one with two neurons (D and E). Each neuron in every layer is linked with all neurons in the neighboring layer. Factor w_{1A} , for instance, denotes the weight of connection between the first neuron in the input layer, X1, and the first neuron of the hidden layer, A. Also the *bias* values of neurons in hidden and output layer are marked with the letter β with lower index of particular neuron.

2.3.3.1 Neuron transfer function

Output of each neuron is given by its transfer function (TF, sometimes called activation function - AF). It ranges between -1 and 1 (in some cases 0 and 1 – use of sigmoid transfer function being one of these cases) and the standard choice is from the following functions:

- linear (the only possibility for input layer),
- sigmoid function,

- hyperbolic tangent, or
- parabolic function.

The argument of each transfer function is a sum of outputs of all neurons from the previous layer which are connected with the neuron, weighted with respective weights, and a specific parameter of the neuron called *bias*.

The input layer has usually only one possibility for transfer function: the linear function. In order to meet the demand of range (-1 to 1, or 0 to 1), the input data must firstly be rescaled. The same process must be applied on the output variables, as well.

The neurons in hidden layers and in the output layer have more options as for the transfer functions. Besides those listed above, any function that maps real numbers onto range of -1 to 1 may be used, although in absolute majority of cases, hyperbolic tangent or sigmoid is used.

Considering the example model depicted on figure 2-12 and hyperbolic tangent TF, the output of the first neuron in the hidden layer is:

$$A = \tanh(X1 \cdot w_{1A} + X2 \cdot w_{2A} + \beta_A), \quad (2-9)$$

where X1 and X2 are scaled values of inputs. Similarly, transfer function of neurons B and C are obtained by simple substitution of B (resp. C) into the last equation. These expressions are subsequently taken as inputs for the output TF, providing:

$$Y = \tanh(A \cdot w_{AY} + B \cdot w_{BY} + C \cdot w_{CY} + \beta_Y), \quad (2-10)$$

2.3.3.2 Training of MLP

In fuzzy logic, two ways were applicable for the creation of model: (1) manual setting of rules, and (2) automatic generation of rules based on datasets. Although it is theoretically possible to define all parameters (weights and biases) of ANN model by hand, it is of no use for practical applications. The parameters are searched for by process called Training.

The main aim of every MLP is to successfully map input dataset into appropriate output data (targets). In order to develop the model, measured (or simulated) input-output datasets must be provided. These data are usually split into three parts of different size: data for training, for test, and for recall [19]. The training dataset is usually the largest of the three and is used to modify the initial model (usually generated randomly). Since capabilities of MLP models are reasonably better in terms of interpolation of data used for training than of extrapolation, it is

important that all boundary datapoints are included in the training part of dataset. The input representing data are propagated through the model and a MLP output is calculated for all the data. The model outputs are compared with the actual outputs from the training datasets and the quality of the model is ordinarily represented either by maximum or mean error.

2.3.3.3 Backpropagation

The common method of this supervised learning is called ‘backward propagation of error’ or ‘backpropagation’ in short. The goal is to find a function that fits a set of inputs to their corresponding outputs. In every step, output of the MLP is calculated using the input data (forward propagation) and error of the model is ascertained. If t stands for target (desired output) and y is MLP output, the error δ is the difference $\delta = t - y$. The problem of learning is thus transformed into optimization problem when the error signal δ is being minimized. This error then propagates the net backwards and brings forth a delta for each neuron in hidden layers as a sum of products of weight of connection leading out of discussed neuron and delta previously calculated for neuron to which the connection leads.

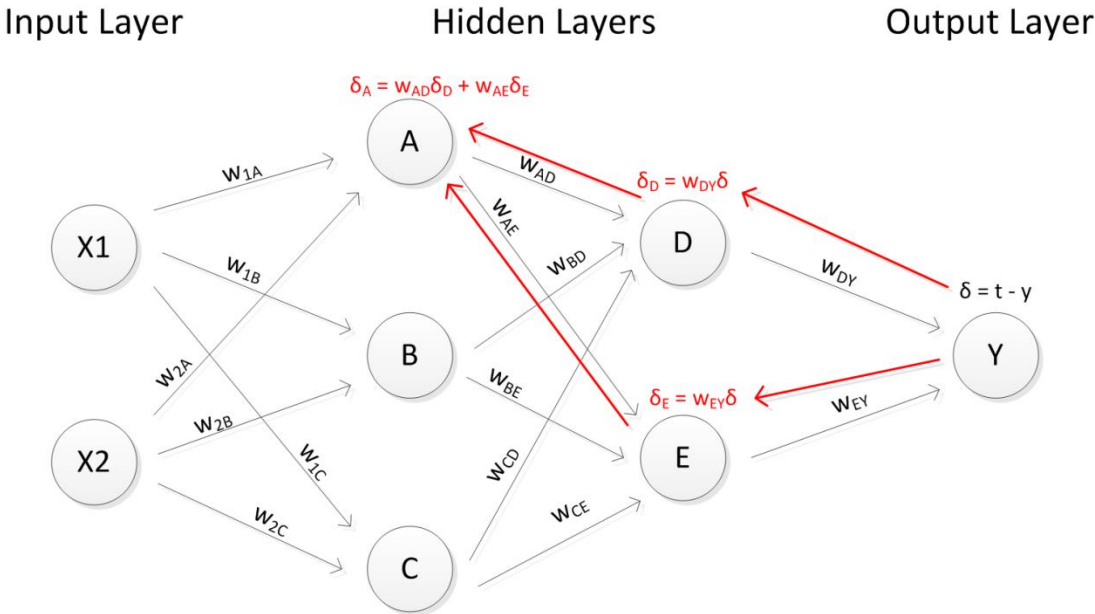


Figure 2-13: Illustration of backward propagation of error

When the error signal δ is determined for all of the neurons (input layer excluding), new weights of all connections are obtained:

$$w'_i = w_i + \eta \delta_i \frac{df_1(e)}{de} x_j, \tag{2-11}$$

where w_i' is new value of weight w_i , η is coefficient or learning rate affecting the speed of training, δ_i is error signal as described above, $\frac{df_1(e)}{de}$ is derivative of neuron activation function and x_j is output of neuron at which the connection originates. The choice of coefficient η is crucial for successful convergence to correct solution. Overly small learning step leads to extensive training time and may converge to local minimum of error, while too large η causes oscillations of found solutions.

2.3.3.4 Test and recall

A test error is calculated for each training iteration. The test data are used similarly as the training ones: the inputs are propagated through the network and a model output is calculated. It is then compared with the desired, actual measured output of the real system and an error, their difference, is determined. Unlike the training data, this error is not used for backpropagation and thus does not affect the weights of the network. The test error is commonly greater than the training error. Therefore the test error is taken as a measure of quality of the model. If the test error exceeds the desired maximum value, a new training must be conducted, possibly with a change of architecture of the MLP.

The recall data are not involved in the training process at all. They are used for the final validation of the model. The recall dataset often consists of a large number of random input data patterns which are propagated through the MLP providing a characteristic map. This approach is of great illustrativeness for system with small number of inputs (< 3) but can be used for more input models as well.

3 Methods for quality evaluation of FM-, TSK- and MLP-models

The error evaluation method is commonly the first one to be used. The models are usually trained with regard to maximum allowed training and test errors and model which does not meet these criteria cannot be considered correct.

Besides the error evaluation, other methods are used including methods based on internal parameters of the model and evaluation based on random values. Basics of these methods are provided in this chapter.

3.1 Model quality analysis based on error values

The evaluation of error is implemented into training of the models (MLP and TSK). The error of training data patterns is being minimized by changing structure (TSK) and parameters (TSK and MLP) of the model until the required criterion is met. Trained model is then (by MLP during the training) tested using different data and again it is explored whether or not the model fulfills the requirements.

Various types of errors are commonly used including:

$$\text{absolute square error: } |E| = \sqrt{(y_{process} - y_{model})^2} \quad (3-1)$$

$$\text{relative square error: } |e| = \frac{\sqrt{(y_{process} - y_{model})^2}}{y_{max} - y_{min}} \quad (3-2)$$

$$\text{absolute mean square error: } |\bar{E}| = \sqrt{\frac{1}{n} \sum_{i=1}^n (y_{process} - y_{model})^2} \quad (3-3)$$

$$\text{and relative mean square error: } |\bar{e}| = \frac{\sqrt{\frac{1}{n} \sum_{i=1}^n (y_{process} - y_{model})^2}}{y_{max} - y_{min}} \quad (3-4)$$

In case that the requirement for maximum error is not known before training, as it was with this thesis, a higher number of different models is trained and their errors compared.

3.2 Model quality analysis based on internal parameters

Analysis of model quality based on internal parameters of the model is only applicable for multilayer perceptrons (parameters are the weights of connections) and Takagi-Sugeno-Kang models (coefficients $b_{x_n c_m}$). The methods are based on comparison of correlation factors (r_{xy}) of real input-output data with coefficients representing linear behavior of the models.

$$r_{xy} = \frac{\sum_{i=1}^n (x_i - \bar{x}) \cdot (y_i - \bar{y})}{\sqrt{\sum_{i=1}^n (x_i - \bar{x})^2 \cdot \sum_{i=1}^n (y_i - \bar{y})^2}} \quad (3-5)$$

The corr. factors represent linearized relationship between two variables (typically an input-output pair). The sign of r_{xy} states the monotony of the relationship, and its absolute value determines the strength of the linear relation as seen on figure 3-1.

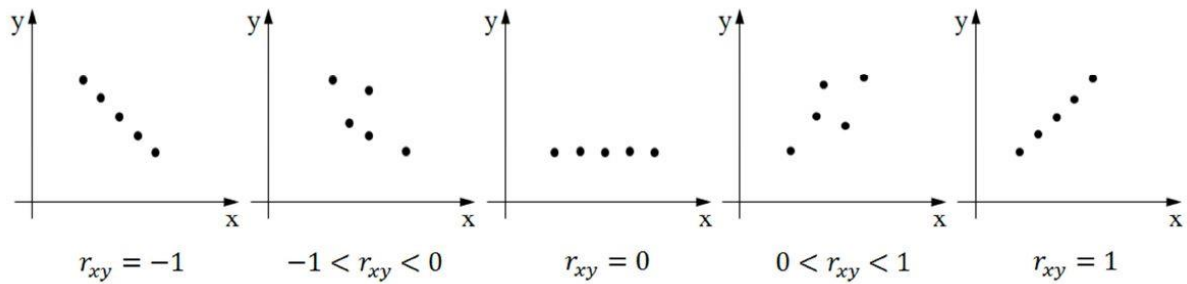


Figure 3-1: Examples of correlation factors [18]

3.2.1 Weight analysis of a MLP model

The first and easy to calculated characteristic of a MLP model is so called **span**. The shape of error surface is dependent on number of connections and their magnitude. The surface becomes more jagged for higher number of connections and for their greater values. The aim of training of MLP is to find the global minimum of error surface but with high jaggedness, the algorithms are more likely to find only one of the local minima, not the global one.

In order to prevent large spans of MLP weights, method of **weight-decay** is applied. This method is an addition to the learning method used in training and its task is to lower down the values of the connections and thus smooth the error surface.

The span is defined as a difference between maximum and minimum value of weights and serves as a first outlook on the model quality with regard to its internal parameters. Lower value of span indicates higher-quality model.

More detailed evaluation of the MLP model quality is via comparison of its correlation coefficients with actual correlation factors of the input-output dataset. The first step of this method is decomposition of the net architecture and linearization of transfer functions. The linearization is performed by substitution of function by series expansion and only the first approximation is considered; in case of hyperbolic tangent TF:

$$\tanh(z) \approx z \quad (3-6)$$

A linear description of input-output relationship is stated:

$$Y_j(X_i) = G_{ij} \cdot X_i + B_j \quad (3-7)$$

where j ranges from 1 to number of outputs, i ranges from 1 to number of inputs, G_{ij} are elements of matrix of weight factors and B_j are elements of vector of biases defined as follows:

For model with 1 hidden layer, G is dot-product of two matrices with coefficients $G_{ij} = F_{ik} \cdot S_{kj}$, where F_{ik} is weight of connection between i -th neuron of input layer and k -th neuron of hidden layer, and S_{kj} is weight of connection between k -th neuron in hidden layer and j -th neuron of the output layer. In case of models with more hidden layers, the matrix G is dot-product of more matrices in analogy.

The vector B is a matrix of biases of neurons in hidden layer weighted by weights of connections and with length equal to number of outputs, $B_j = \sum_i \beta_i \cdot w_{i,Y_j} + \beta_{Y_j}$. This vector is out of importance for the weight analysis of MLP model.

In order to compare the weight factors G_{ij} with the correlation factors r_{xy} , the weights factors are normalized into correlation weights Ψ :

$$\Psi_{ij} = \frac{G_{ij}}{\sqrt{\sum G_{ij}^2}} \quad (3-8)$$

Both these coefficients, correlation weights and correlation factors, describe linear relationship between input and output variables. The sign of the coefficients determines the monotony of the linear relation (negative: decreasing, positive: increasing) and the absolute value characterizes its intensity.

3.2.2 Correlation analysis of a TSK-model

The linear input-output dependency is directly represented in the linear part of TSK-model (sect. 2.3.2.1). Coefficient F_{xy} is calculated for each input-output variable pair:

$$F_{xy} = \sum_m b_{x_n} c_m \quad (3-9)$$

and is then normalized to match the correlation factors:

$$K_{xy} = \frac{F_{xy}}{\sqrt{\sum_n F_{xy}^2}} \quad (3-10)$$

A concurrence between normalized degrees of linear relationship of the model K_{xy} and correlation coefficients r_{xy} is analyzed.

3.3 Model quality analysis based on random numbers

This method makes use of what was called ‘recall’ in sect. 2.3.3.4. A large dataset containing random values is produced; number of data in each data pattern corresponds to number of inputs of the model. These data patterns are then propagated through the net one by one, and respective MLP outputs are calculated.

The combination of such input and output data generates a characteristic map which is easy to be visually analyzed and the correctness of model assessed. This approach is particularly relevant for models with one or two outputs when the characteristic map is a 2-D or 3-D graph respectively.

4 Development of models

In this chapter, a principal part of the thesis – the development of SC models – is described. Using general knowledge from sect. 2.3, five different soft computing models are to be produced: Fuzzy model by Mamdani, two MLP models (one with 1 hidden layer, one with 2), and two TSK models (see sect. 4.5). A higher number of models of each kind (except for Mamdani) will be developed in order to compare different architectures (numbers of neurons and their TFs for MLP, and number of clusters for TSK). Furthermore, a quality analysis of the models based on methods from previous chapter is to be performed, and the best-choice model of each type chosen.

The main motivation for this work is to find out which of the discussed SCM is the most suitable for classification of the core states. Properties of the models as well as some issues related to their use for the core diagnosis are to be investigated.

The general method for investigations is depicted on figure 4-1. The dataset is described in the following section in detail.

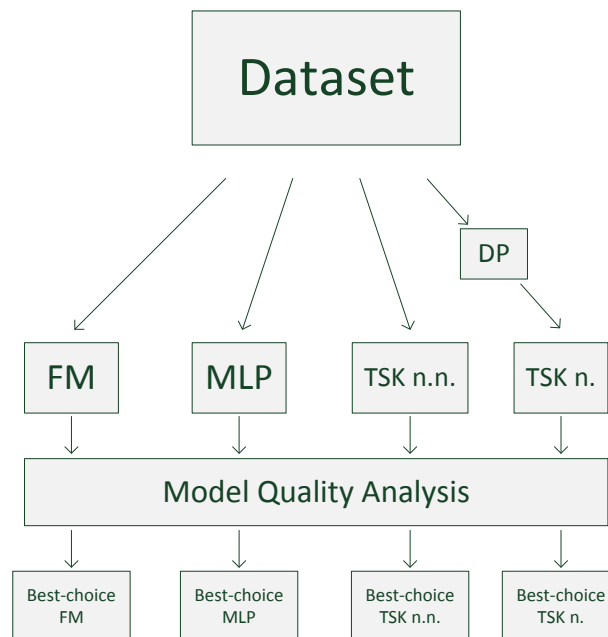


Figure 4-1: Schema of general method for investigations

In figure 4-1, the DP block stands for data processing (normalization of the data, see sect. 4.5.2), TSK n.n. means Takagi-Sugeno-Kang model trained using not normalized data, TSK n., in parallel, is TSK model with use of normalization. Model quality analysis is performed, depending on particular model type and according to methods described in sect. 3.

As a result of the models development, a total of five different models fulfilling the criteria from section 4.2 are expected. The models will further be investigated in terms of their sensitivity.

4.1 Description of datasets

For development of SC models, training and test datasets must be provided. In the standard way, the data are obtained from the real system measurement. However, it is not possible to get the real data for this project since there were only two actual core meltdowns in LWR (TMI-2 and Fukushima) and there were no gamma distribution measurements outside the RPV there. Initiation of another core meltdown in a NPP is not possible from the safety point of view. For use in this project, artificial data need to be generated.

Generation of the datasets required for creation of SCMs is based on postulated development of gamma distribution during a low-pressure scenario of core meltdown (see sect. 2.2.4). It consists of 10 significant states in total: standard operation (normal) state, 3 states describing the early in-vessel phase, and 6 states for the late in-vessel phase.

A great disadvantage of such manually produced data is obvious: There is no knowledge whether the datasets or curves of gamma distribution respectively are absolutely correct. Also no background noise is introduced and thus there is only one line corresponding to each state. On the other hand, these disadvantages are not necessarily relevant for this thesis. As it was mentioned above, its main objective is not to develop one concrete model but rather to investigate the general suitability of SCMs for the classification of the core meltdown states.

Several assumptions were made regarding physical configuration of the measurement chain:

- The overall height of the measuring rod reaching from upper edge of the reactor core to the lower plenum of RPV is 7 meters.
- There are 15 sensors in the rod, providing 0.5-meter spacing between them.
- The maximum activity measured by sensor is 10,000 impulses/s.

Besides the training and test datasets for the very development of the models, recall datasets must be generated as well, in order to validate the quality of said models. The description of all datasets is provided in following sections.

4.1.1 Training and test datasets

Using postulated gamma distribution (figure 2-3) and the assumptions from previous section, the training data set was produced. The activities ‘measured’ by each sensor in respective core state are stated in table 4-1 and table 4-2. Figure 4-2 shows the produced training data in a 3-D plot.

Sensor no.	Height [m]	Activity [1/s]				
		State 0	State 1	State 2	State 3	State 4
1	7.0	1000.0	3000.0	3000.0	3500.0	1000.0
2	6.5	2100.0	4500.0	4600.0	5100.0	5200.0
3	6.0	3000.0	5000.0	5600.0	6100.0	6200.0
4	5.5	3600.0	4600.0	6000.0	6100.0	6300.0
5	5.0	3900.0	4200.0	5850.0	6000.0	6100.0
6	4.5	4000.0	4000.0	5400.0	5600.0	5700.0
7	4.0	3900.0	3900.0	4800.0	5000.0	5100.0
8	3.5	3600.0	3600.0	4000.0	4200.0	4300.0
9	3.0	3000.0	3000.0	3100.0	3300.0	3400.0
10	2.5	2100.0	2100.0	2100.0	2200.0	2300.0
11	2.0	1000.0	1000.0	1000.0	1000.0	1100.0
12	1.5	0.0	0.0	0.0	0.0	100.0
13	1.0	0.0	0.0	0.0	0.0	0.0
14	0.5	0.0	0.0	0.0	0.0	0.0
15	0.0	0.0	0.0	0.0	0.0	0.0

Table 4-1: Training data for development of models (part 1/2)

Sensor no.	Height [m]	Activity [1/s]				
		State 5	State 6	State 7	State 8	State 9
1	7.0	1000.0	1000.0	1000.0	1000.0	1000.0
2	6.5	1500.0	1500.0	1500.0	1500.0	1500.0
3	6.0	1500.0	1500.0	1500.0	1500.0	1500.0
4	5.5	6100.0	1500.0	1500.0	1500.0	1500.0
5	5.0	7200.0	6800.0	1500.0	1500.0	1500.0
6	4.5	7500.0	7900.0	6800.0	1500.0	1500.0
7	4.0	7600.0	8200.0	7900.0	1500.0	1500.0
8	3.5	7800.0	8300.0	8200.0	1500.0	1500.0
9	3.0	7400.0	8700.0	8300.0	1500.0	1500.0
10	2.5	5900.0	8300.0	8700.0	1500.0	1500.0
11	2.0	2800.0	5800.0	8200.0	2500.0	2500.0
12	1.5	100.0	100.0	6400.0	8800.0	7500.0
13	1.0	0.0	0.0	2400.0	10000.0	10000.0
14	0.5	0.0	0.0	1700.0	8800.0	9500.0
15	0.0	0.0	0.0	1500.0	4000.0	6000.0

Table 4-2: Training data for development of models (part 2/2)

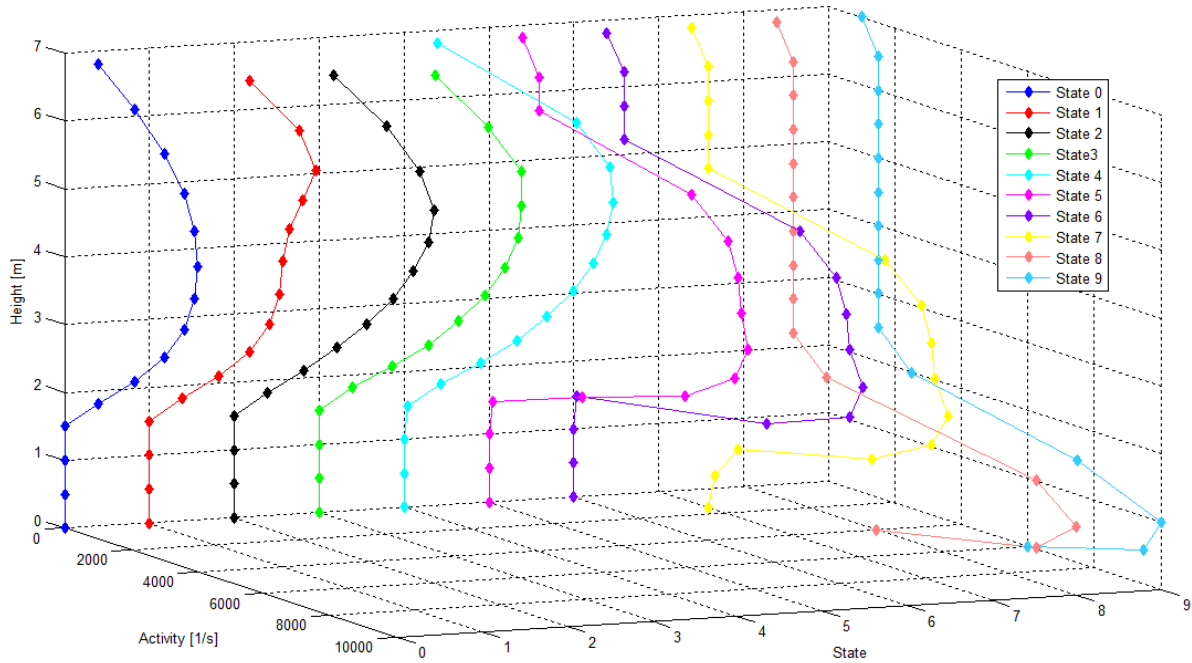


Figure 4-2: 3-D plot of training dataset produced based on postulated core states during core meltdown

The maximum considered activity is 10,000 impulses/s. These highest peaks are recorded in the final states by the sensors in the lower plenum. Important characteristics, later to be used for models quality evaluation, are the correlation factors, describing the linear relationship between individual inputs and the output. The factors are shown in table 4-3, where $r_{x_i y}$ is a corr. factor of i -th input to the output.

$r_{x_1 y}$	$r_{x_2 y}$	$r_{x_3 y}$	$r_{x_4 y}$	$r_{x_5 y}$	$r_{x_6 y}$	$r_{x_7 y}$	$r_{x_8 y}$
-0.489	-0.524	-0.585	-0.568	-0.401	-0.124	-0.022	0.068
$r_{x_9 y}$	$r_{x_{10} y}$	$r_{x_{11} y}$	$r_{x_{12} y}$	$r_{x_{13} y}$	$r_{x_{14} y}$	$r_{x_{15} y}$	
0.182	0.315	0.571	0.755	0.699	0.689	0.712	

Table 4-3: Correlation factors of generated training data

The training data can be used for training of all SC models. In order to develop a MLP- and TSK-models, training and **test** dataset must be provided. The test data were obtain by interpolation between convenient ‘training’ states, i.e. gamma distribution of a new state was estimated so that it lies in between two neighboring states produced above. An example of test data production is provided in table 4-4, where there are two ‘test’ states created between normal operation state (state 0) and the first state of the early phase (state 1). The notation of both training and test states was remade in such way that all these states are denoted by an integer in an ascending order (as seen in table 4-4). The graphical representation of table 4-4 data is provided on figure 4-3.

Sensor no.	Height [m]	Activity [1/s]			
		State 0	1 st test st.	2 nd test st.	State 1
1	7.0	1000.0	1600	2200	3000.0
2	6.5	2100.0	2800	3900	4500.0
3	6.0	3000.0	3700	4300	5000.0
4	5.5	3600.0	4100	4200	4600.0
5	5.0	3900.0	4050	4100	4200.0
6	4.5	4000.0	4000.0	4000.0	4000.0
7	4.0	3900.0	3900.0	3900.0	3900.0
8	3.5	3600.0	3600.0	3600.0	3600.0
9	3.0	3000.0	3000.0	3000.0	3000.0
10	2.5	2100.0	2100.0	2100.0	2100.0
11	2.0	1000.0	1000.0	1000.0	1000.0
12	1.5	0.0	0.0	0.0	0.0
13	1.0	0.0	0.0	0.0	0.0
14	0.5	0.0	0.0	0.0	0.0
15	0.0	0.0	0.0	0.0	0.0
Former state notation:		0	-	-	1
New state notation:		0	1	2	3

Table 4-4: Example of test dataset creation – interpolation between state 0 and state 1

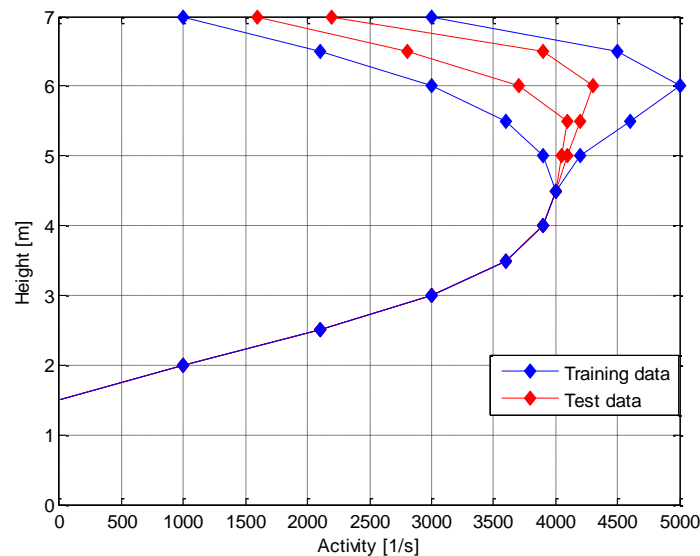


Figure 4-3: Graphical interpretation of data from table 4-4

Similarly, test data were produced by interpolation between states 1 and 2 (two data patterns), 2 and 3, 3 and 4, 5 and 6, 6 and 7, and between states 8 and 9 (always one data pattern). The notation of states was shifted with respect to newly created ‘test’ states, as seen in table 4-4. This way, a complete dataset with 19 states was produced with 10 training- and 9 test data patterns (figure 4-4).

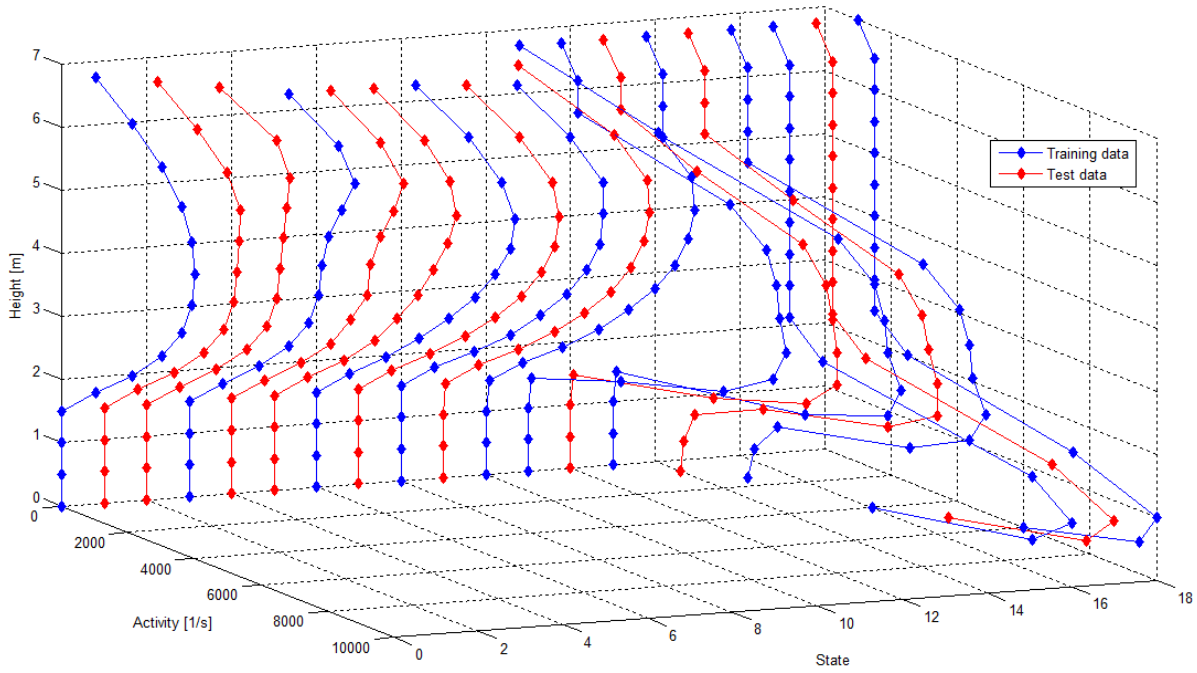


Figure 4-4: Graphical illustration of training (blue) and test (red) datasets

The complete test dataset can be found in the appendix and on the data-CD.

4.1.2 Recall datasets for validation of SCMs

In addition, total of three recall datasets were produced. As mentioned in sect. 2.3.3.4, these datasets contain a large number of data patterns (300 in this case) consisting of random numbers. The first recall data file was created using absolutely random values between 0 and 10,000 imp/s for all inputs. In the second dataset, values of training data for individual inputs were taken into account and the random values for each input ranges between minimum value minus 1,000 imp/s and maximum value plus 1000 imp/s. Lastly the third recall dataset was produced with respect to defined ‘training’ states. For each state (10), thirty random vectors of inputs were generated where the input values vary around the actual value for given state and sensor with range of ± 500 imp/s.

The complete recall datasets can be found on the data-CD.

4.2 Error limits and decision criteria for the investigations

Since there is no physical connection between gamma distribution and the notation of states and the models are trained only using the training data, the test errors are expected to be

significantly greater than the training ones. It also cannot be decided which model is of higher quality based on the test errors. Yet the test error criteria provide highly important information since the model which fails them cannot be taken as a suitable model.

There are two ‘test’ states (state 1 and state 2) between the first two ‘training’ states (state 0 and state 3). The test errors are assessed in such way that model outputs for these test states must lie between 0 and 3 (in an open interval) and the output for data of state 2 must be greater than the output for those of state 1. Similarly it is dealt with test states 4 and 5. In other cases, there is only one test state between two training states, and the requirements for their respective output is thus reduced to that the absolute value of the error must be smaller than 1.

Quality of MLP and TSK models can be indicated by their structure – value of weights (MLP) and coefficients (TSK). High absolute values of those as well as a large difference between maximum and minimum values imply poor quality.

The linearized behavior of the models (MLP and TSK) is to be studied next. Correlation weights (MLP) and correlation coefficients (TSK) are to be compared with empirical correlation factors of the training dataset. A model with higher degree of concurrence is considered to be of higher quality.

Finally, a quality analysis based on random vectors (recall datasets) is to be performed. Results for recall dataset no. 3 are of particular interest, since they can be compared with the original state used for generation of the ‘random’ data.

4.3 Development of fuzzy model by Mamdani (FM)

General properties and design procedure of a FM model is noted in sect. 2.3.1. Only the training data were used for the development of the model. Set of rules was established according to eq. (2-1), one rule for each state. The data base contains 15 input- and one output variable; each variable incorporating one triangular membership function for every significant value of individual input from the training set, as depicted on figure 4-5.

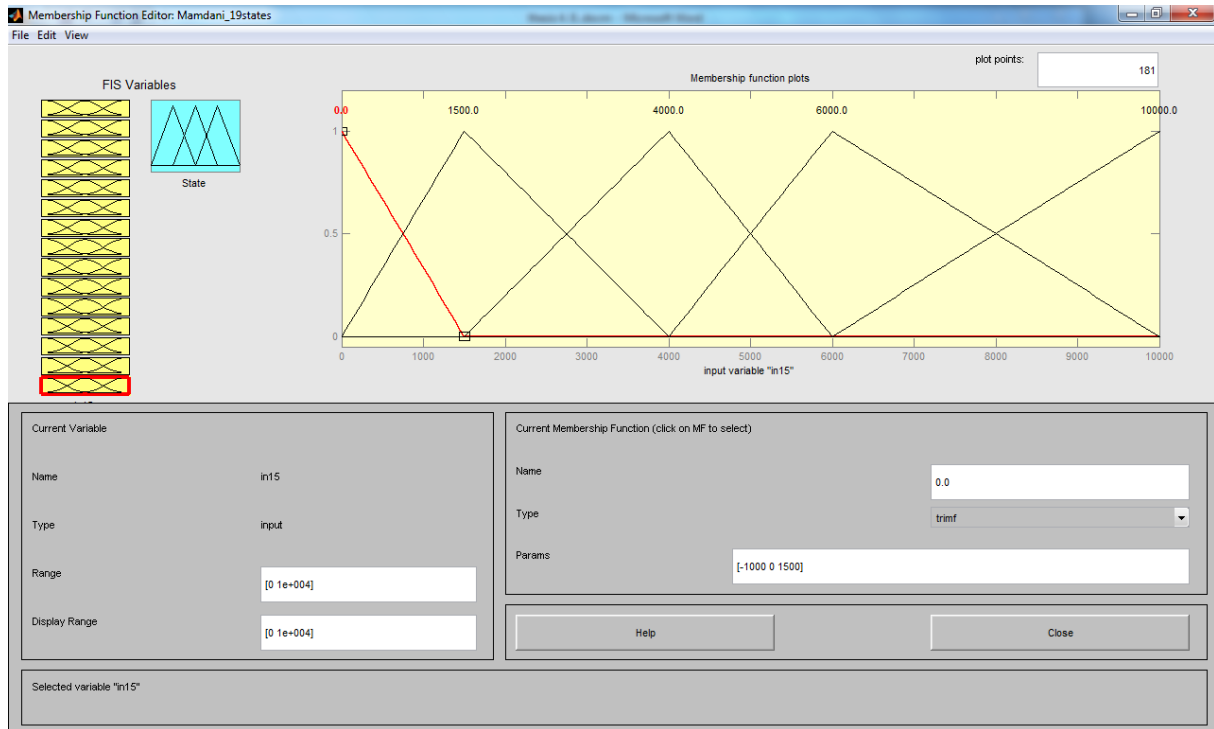


Figure 4-5: Membership functions of input no. 15

The rule base was created according to following paradigm:

R_i : IF *input1* is (*value of input1 in state i*) AND ... AND *input15* is (*value of input15 in state i*) THEN *state* is *state i*.

The methods of operators were chosen as for typical Mamdani system:

AND method: *minimum*

OR method: *maximum*

Implication: *minimum*

Aggregation: *maximum*

Defuzzification: *COG*

4.3.1 Quality analysis of FM model

Test data and the three recall datasets described at the end of sect. 4.1 were used for assessment of the model quality. Since the model is characterized only by the fuzzy rules, and thus contains no internal parameters, other model quality analysis methods (sect. 3.2) are not applicable.

The first evaluation was performed using the training data; the model outputs were calculated for each training data pattern:

Index of tr. input	Expected output *)	Output of FM model	Difference
1	0	0.278	0.278
2	3	3.001	0.001
3	6	5.999	-0.001
4	8	7.998	-0.002
5	10	10.006	0.006
6	11	10.999	-0.001
7	13	12.999	-0.001
8	15	14.999	-0.001
9	16	16.001	0.001
10	18	17.717	-0.283

Table 4-5: Evaluation of FM model based on training data

*) The value of expected output is determined by the state set for respective input vector in the rule base.

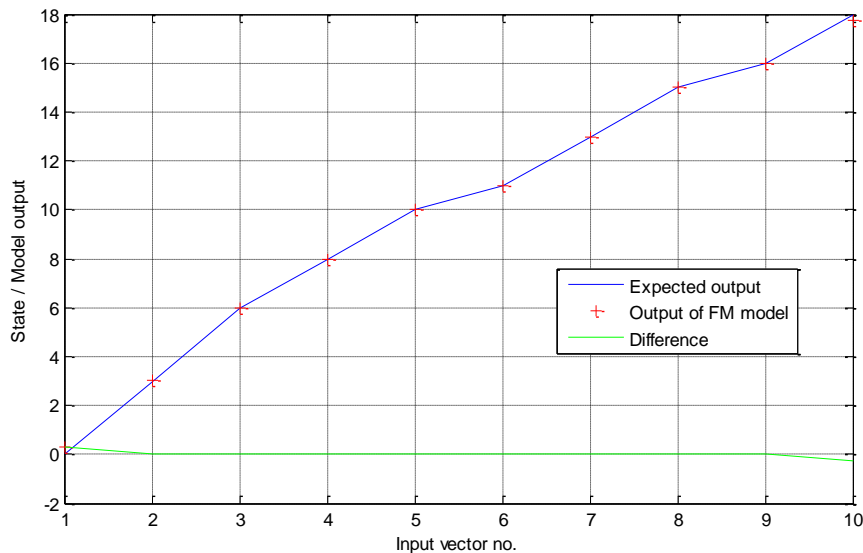


Figure 4-6: Graphical representation of data from table 4-5 (training errors of the FM model)

The test data were also evaluated by the FM model and following results were obtained:

Index of test input	Expected output **)	Output of FM model	Difference
1	1	1,13	0,13
2	2	2,42	0,42
3	4	3,70	-0,30
4	5	4,74	-0,26
5	7	6,84	-0,16
6	9	8,78	-0,22
7	12	12,02	0,02
8	14	13,96	-0,04
9	17	16,59	-0,41

Table 4-6: Evaluation of FM model based on test data

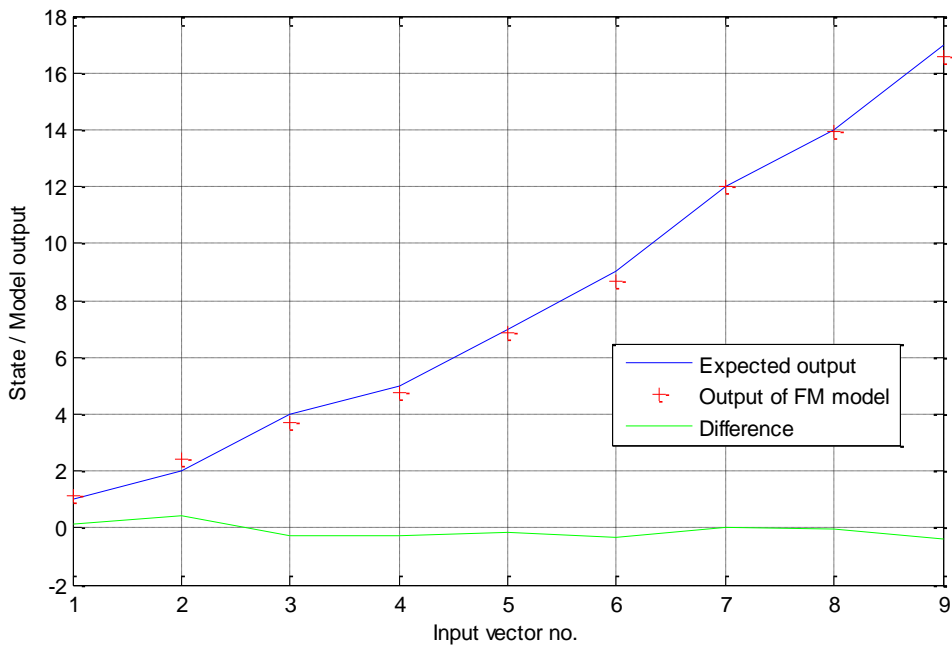


Figure 4-7: Graphical representation of data from table 4-6 (test errors of the FM model)

**) Value of expected output corresponds to notation of states as indicated in table 4-4. It is not determined by any physical nature of the process and thus it is not supposed that the model outputs would perfectly match the ‘expected’ outputs. The absolute value of their difference, however, should not exceed 1 as this would indicate that the model was unable to correctly classify the state which lies between set ‘training’ states. In cases there were two test states defined between two consecutive training states, the error is allowed to be greater than 1, yet the model outputs must lie in an open interval between the training states and the order of the test states must be kept (i.e. output of the model for input vector with higher index must be greater than outputs obtained by input vectors with lower indices).

Also the random data based analysis was conducted using recall datasets (sect. 4.1). For completely random values (recall data no. 1) and random data reflecting only range of values for individual inputs (recall data no. 2), it was expected (and subsequently confirmed) that the strength of all rules from the rule base would be 0. Center-of-Gravity method was chosen as a defuzzification method, and the range of the output variable is 0–18. When no rule forms the output fuzzy set, the algorithm returns center the range, in this case 9, as an output.

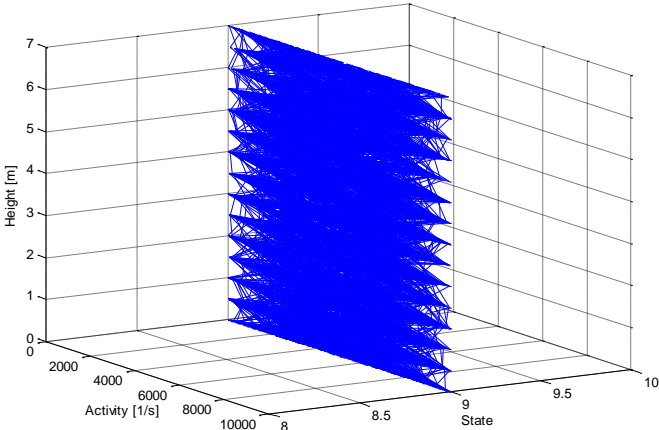


Figure 4-8: Analysis of FM model based on random values (recall data 1) – all input vectors are classified as state 9.

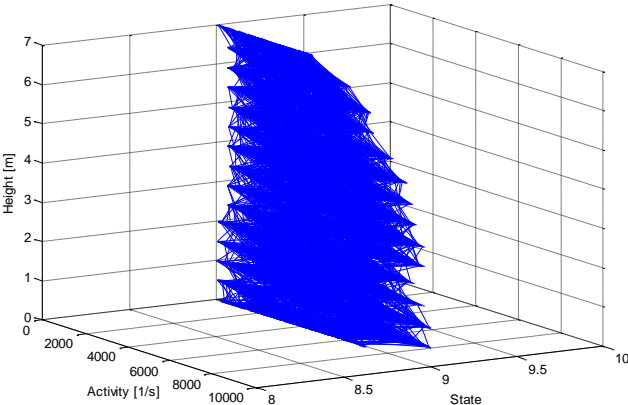


Figure 4-9: Analysis of FM model based on random values (recall data 2) – all input vectors are classified as state 9.

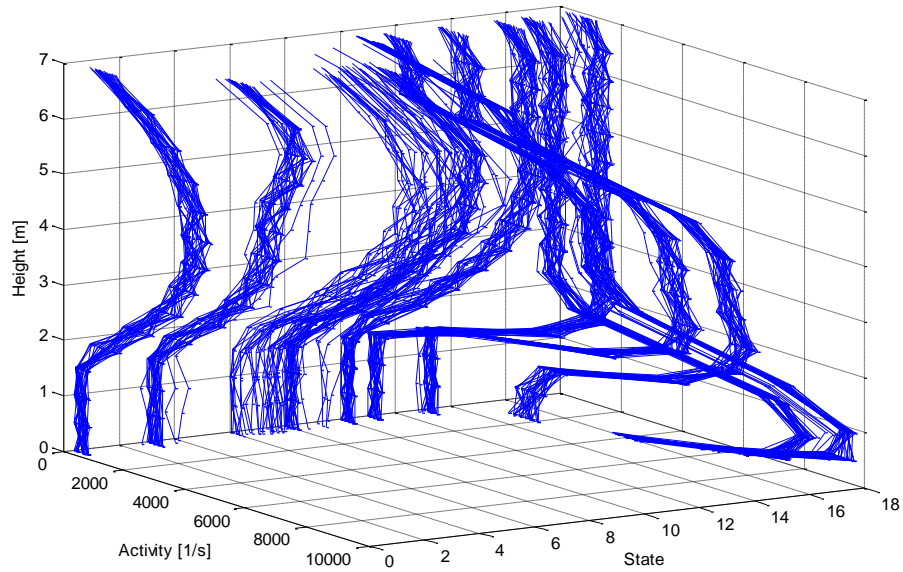


Figure 4-10: Analysis of FM model based on random values (recall data 3) – model correctly classifies most of the input vectors

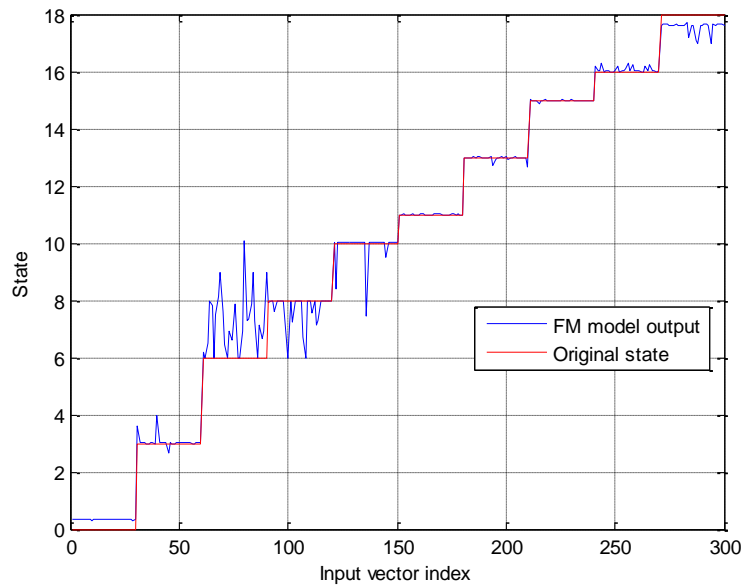


Figure 4-11: Comparison of FM model outputs and original states used for generation of random values

The corrugation between states 6 and 10 could be expected as there are only small differences (smaller than the range of 500) among input values characteristic for these states. There were totally 3 input vectors generating output 9 – the truth value for premises of each rule is 0.

The overall quality of developed FM model is good. The connections between individual expressions in the premise part are AND, which signifies that if the truth value of as few as one of them is 0, the ADOM of the antecedent is 0 and the rule is not valid. This in combination

with random input vectors causes zero output fuzzy set and the algorithm returns 9 (the center of output variable range) as an output.

4.4 Development of MLP models

Artificial neural network models in form of multilayer perceptron were trained. Training and test datasets as described in sect. 4.1 were used for the development, and the recall data for final assessment of their quality. In addition, weight analyses of the models were conducted.

Since it cannot be decided in advance which architecture is the most suitable to be used, a larger number of MLPs with different structures were produced. The investigation were performed in DataEngine program where there are two options for number of hidden layers – one or two HLs. A total of 10 models with 1 HL and different transfer functions, and the same number of models with 2 hidden layers were trained (see table 4-7Table 4-7).

The approximate number of neurons in HLs was determined by means of **pruning**. This method is used for simplification of large MLP nets. It dismisses the least significant connections, i.e. connections with the smallest weights. The required complexity of MLP model is then characterized by number of connections at the end of training with pruning activated. The resultant net contain higher number of neurons is hidden layers than necessary and thus a new MLP is to be trained whose number of connections correspond with the previous one but number of neurons is significantly lower (and pruning deactivated).

Model no.	No. of HLs	1 st HL neurons	1 st HL TF	2 nd HL neurons	2 nd HL TF	Output TF	Max. tr. error	Average tr. error	Max. test error	Average test error
1	1	3	tanh	–	–	lin.	0.040	0.012	0.745	0.242
2	1	3	tanh	–	–	sigm.	0.280	0.059	0.625	0.261
3	1	3	sigm.	–	–	tanh	0.199	0.043	0.596	0.322
4	1	5	lin.	–	–	tanh	0.217	0.041	0.660	0.248
5	1	5	tanh	–	–	sigm.	0.274	0.059	0.643	0.248
6	1	5	sigm.	–	–	lin.	0.190	0.047	0.463	0.201
7	1	8	lin.	–	–	sigm.	0.380	0.082	0.682	0.209
8	1	8	sigm.	–	–	lin.	0.121	0.029	0.577	0.238
9	1	8	tanh	–	–	tanh	0.098	0.021	0.680	0.330
10	1	15	tanh	–	–	lin.	0.014	0.003	0.689	0.251
11	2	3	sigm.	3	tanh	sigm.	0.314	0.070	0.626	0.251
12	2	5	tanh	4	tanh	tanh	0.084	0.017	0.759	0.393
13	2	4	sigm.	5	sigm.	lin.	0.094	0.022	0.529	0.208
14	2	6	lin.	6	lin.	lin.	0.012	0.006	0.794	0.203
15	2	7	tanh	2	lin.	sigm.	0.177	0.036	0.624	0.291
16	2	7	sigm.	3	tanh	sigm.	0.309	0.068	0.646	0.242
17	2	8	tanh	5	sigm.	tanh	0.128	0.027	0.696	0.362
18	2	8	tanh	8	tanh	lin.	0.010	0.002	0.628	0.240
19	2	9	sigm.	7	lin.	tanh	0.123	0.027	0.613	0.304
20	2	12	sigm.	11	sigm.	tanh	0.266	0.051	0.650	0.269

Table 4-7: Overview of architectures of all trained MLPs and their respective errors

The error based analyses show that all of the models fulfill the requirements (sect 4.2). The properties of errors are similar to what applied to errors by FM model. Although the model should be able to classify training input vectors correctly (i.e. the training errors should be minimum), the test errors are allowed to be greater but not more than 1 (in most cases, see sect. 0 for more info), as it would imply wrong classification of the test input vector. All models satisfy these criteria, although some differences may be observed.

4.4.1 Weight analysis of MLP models

Quality analysis based on internal parameters of the models was performed. Firstly statistical properties of the weights, especially the values of span, were inspected.

Model no.	Variance	Maximum	Minimum	Span	Average
1	0.054	0.361	-0.992	1.353	-0.137
2	0.341	0.249	-2.505	2.754	-0.379
3	1.055	3.755	-4.282	8.036	-0.040
4	0.176	0.575	-1.757	2.332	-0.091
5	0.256	2.213	-1.451	3.664	0.132
6	0.133	1.763	-0.875	2.638	0.114
7	0.133	1.139	-1.894	3.033	-0.102
8	0.095	2.027	-0.807	2.834	0.059
9	0.101	0.830	-1.751	2.581	-0.085
10	0.031	1.017	-0.566	1.583	0.029
11	0.710	3.084	-2.746	5.829	0.005
12	0.137	1.102	-1.213	2.316	-0.087
13	0.463	2.787	-1.981	4.768	-0.398
14	0.069	0.641	-0.829	1.470	0.008
15	0.129	2.104	-1.210	3.314	-0.029
16	0.310	3.157	-1.948	5.106	0.001
17	0.190	1.732	-1.916	3.647	0.062
18	0.039	0.808	-0.698	1.506	-0.019
19	0.135	1.126	-1.802	2.928	-0.067
20	0.178	1.904	-1.382	3.286	-0.260

Table 4-8: Statistical properties of weights of the MLP models

Since weight-decay was activated for training of the models, the absolute values of all weights are generally small. The maximum value of span 8.036 (model no. 3) still implies a good quality of the model.

Furthermore, a weight analysis by means of correlation weights comparison was made. The weights of each model were transformed into matrices required for calculation of weight factor vectors G_i , as described in sect. 3.2.1. Next, the correlation weights Ψ_i were calculated according to formula (3-8) and compared with empirical correlation factors.

	MLP 1	MLP 2	MLP 3	MLP 4	MLP 5	MLP 6	MLP 7	CORR
Ψ_1	-0.057	0.004	-0.009	-0.011	0.004	-0.075	-0.021	-0.489
Ψ_2	0.120	0.386	0.384	0.393	0.397	0.179	0.414	-0.524
Ψ_3	0.288	-0.037	-0.042	-0.200	-0.051	0.246	-0.118	-0.585
Ψ_4	-0.249	0.118	0.127	0.206	0.120	-0.199	0.155	-0.568
Ψ_5	0.049	0.188	0.160	0.233	0.211	0.155	0.226	-0.401
Ψ_6	0.284	0.018	0.018	-0.115	0.029	0.237	-0.030	-0.124
Ψ_7	0.279	0.021	0.027	-0.102	-0.012	0.262	-0.021	-0.022
Ψ_8	0.334	0.106	0.096	-0.065	0.102	0.328	0.024	0.068
Ψ_9	0.360	0.185	0.175	0.054	0.197	0.319	0.168	0.182
Ψ_{10}	0.063	0.236	0.238	0.314	0.239	0.066	0.277	0.315
Ψ_{11}	-0.260	0.151	0.159	0.382	0.163	-0.176	0.238	0.571
Ψ_{12}	0.228	-0.111	-0.125	-0.157	-0.090	0.268	-0.113	0.755
Ψ_{13}	0.335	0.226	0.205	0.108	0.229	0.368	0.226	0.699
Ψ_{14}	0.331	0.353	0.329	0.214	0.356	0.362	0.338	0.689
Ψ_{15}	0.302	0.699	0.721	0.593	0.678	0.361	0.631	0.712
sum of errors	6.612	5.641	5.645	5.825	5.627	6.408	5.520	

Table 4-9: Correlation weights of MLP models compared with empirical correlation factors of input data (part 1/3)

	MLP 8	MLP 9	MLP 10	MLP 11	MLP 12	MLP 13	MLP 14	CORR
Ψ_1	-0.068	0.027	-0.058	0.015	-0.014	-0.060	-0.048	-0.489
Ψ_2	0.164	0.388	0.185	0.395	0.424	0.270	0.089	-0.524
Ψ_3	0.270	-0.029	0.211	-0.043	-0.025	0.201	0.251	-0.585
Ψ_4	-0.255	0.117	-0.289	0.128	0.061	-0.152	-0.189	-0.568
Ψ_5	0.123	0.180	0.140	0.197	0.110	0.208	0.033	-0.401
Ψ_6	0.287	0.009	0.275	0.008	0.014	0.248	0.197	-0.124
Ψ_7	0.278	0.019	0.267	0.045	0.068	0.210	0.229	-0.022
Ψ_8	0.321	0.123	0.333	0.088	0.167	0.276	0.359	0.068
Ψ_9	0.314	0.198	0.399	0.169	0.226	0.324	0.365	0.182
Ψ_{10}	0.070	0.248	0.072	0.222	0.248	0.163	-0.109	0.315
Ψ_{11}	-0.138	0.105	-0.152	0.165	0.153	-0.010	-0.502	0.571
Ψ_{12}	0.246	-0.135	0.233	-0.115	-0.133	0.277	0.215	0.755
Ψ_{13}	0.343	0.222	0.367	0.232	0.171	0.391	0.304	0.699
Ψ_{14}	0.364	0.319	0.295	0.342	0.325	0.392	0.306	0.689
Ψ_{15}	0.346	0.711	0.304	0.698	0.695	0.344	0.204	0.712
sum of errors	6.407	5.766	6.546	5.689	5.777	6.172	7.071	

Table 4-10: Correlation weights of MLP models compared with empirical correlation factors of input data (part 2/3)

	MLP 15	MLP 16	MLP 17	MLP 18	MLP 19	MLP 20	CORR
Ψ_1	0.020	0.021	0.014	-0.057	0.045	0.061	-0.489
Ψ_2	0.404	0.399	0.343	0.228	0.398	0.424	-0.524
Ψ_3	-0.065	-0.057	-0.035	0.198	-0.018	-0.039	-0.585
Ψ_4	0.120	0.131	0.123	-0.224	0.133	0.130	-0.568
Ψ_5	0.204	0.211	0.179	0.153	0.202	0.237	-0.401
Ψ_6	-0.002	-0.018	0.037	0.259	-0.003	-0.009	-0.124
Ψ_7	0.054	0.011	0.031	0.220	0.033	0.024	-0.022
Ψ_8	0.093	0.085	0.076	0.316	0.122	0.105	0.068
Ψ_9	0.177	0.195	0.161	0.353	0.194	0.197	0.182
Ψ_{10}	0.203	0.226	0.220	0.120	0.212	0.239	0.315
Ψ_{11}	0.162	0.172	0.188	-0.116	0.127	0.150	0.571
Ψ_{12}	-0.118	-0.119	-0.148	0.194	-0.126	-0.071	0.755
Ψ_{13}	0.214	0.222	0.180	0.336	0.201	0.253	0.699
Ψ_{14}	0.342	0.337	0.309	0.401	0.349	0.350	0.689
Ψ_{15}	0.699	0.687	0.752	0.390	0.698	0.649	0.712
sum of errors	5.718	5.657	5.754	6.326	5.849	5.765	

Table 4-11: Correlation weights of MLP models compared with empirical correlation factors of the input data (part 3/3)

The sum of errors is calculated as follows:

$$\text{sum of errors} = \sum_{i=1}^{15} |\Psi_i - r_i| \quad (4-1)$$

where r_i is correlation factor corresponding to correlation weight Ψ_i .

One can observe large differences between correlation weights of MLPs and the empirical corr. factors. In order to make the model quality evaluation, not only the absolute difference between Ψ_i and r_i is of interest. Firstly the signs of both should match as they determine the monotony of the linear relationship.

The high level of mismatch of the compared values is most likely caused by a strong nonlinearity of the output-input relationship. Although, there can be found some models with higher concurrence. In case of MLP 7, the sign differs in only four rows and the sum of errors is the least of all models. MLP 16 is the best 2HL model according to weight analysis. Both these models (MLP 7 and 16) also have reasonably small training and test errors, and thus can be considered the best MLP models.

4.4.2 Quality analysis of MLP models based on random values

MLP models no. 7 and 12, chosen as the best MLP models based on internal parameters analysis, were further investigated using recall datasets. Only results for the third dataset are provided as no relevant information can be read easily from the first two.

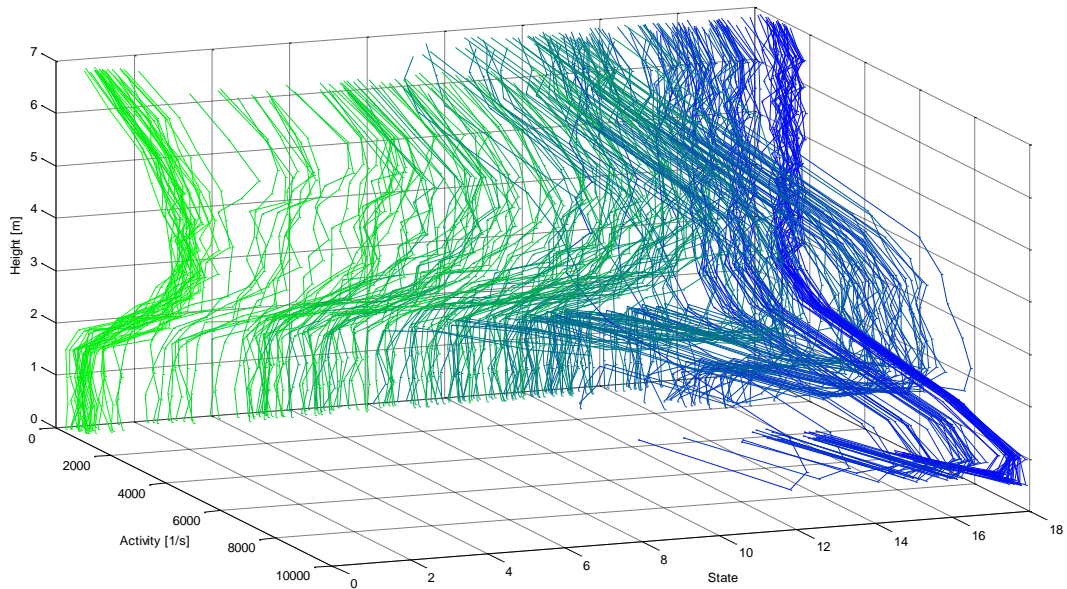


Figure 4-12: Analysis of MLP model no. 7 based on random values (recall data 3). The color of line determines index of the input vector – the first one green, the last one blue; the RGB value changes linearly

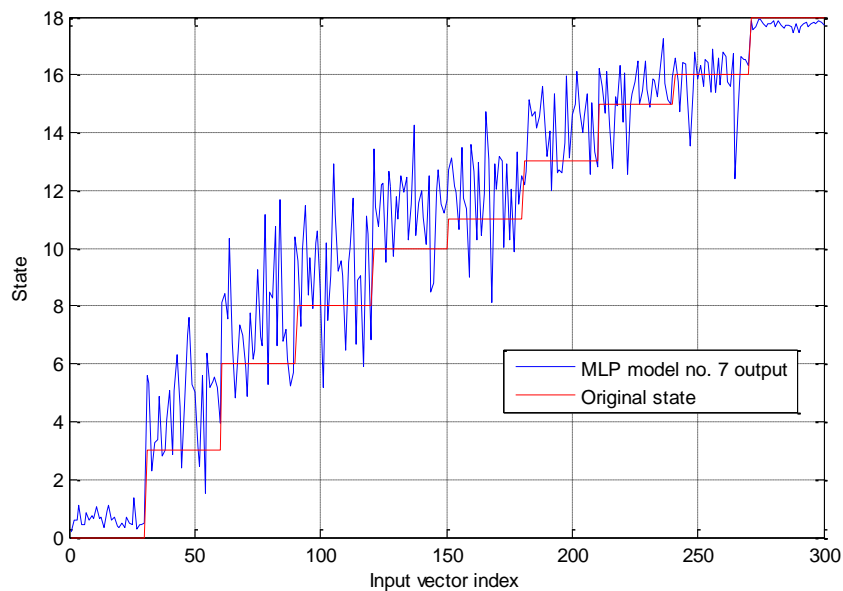


Figure 4-13: Comparison of MLP model no. 7 outputs and original states used for generation of random values

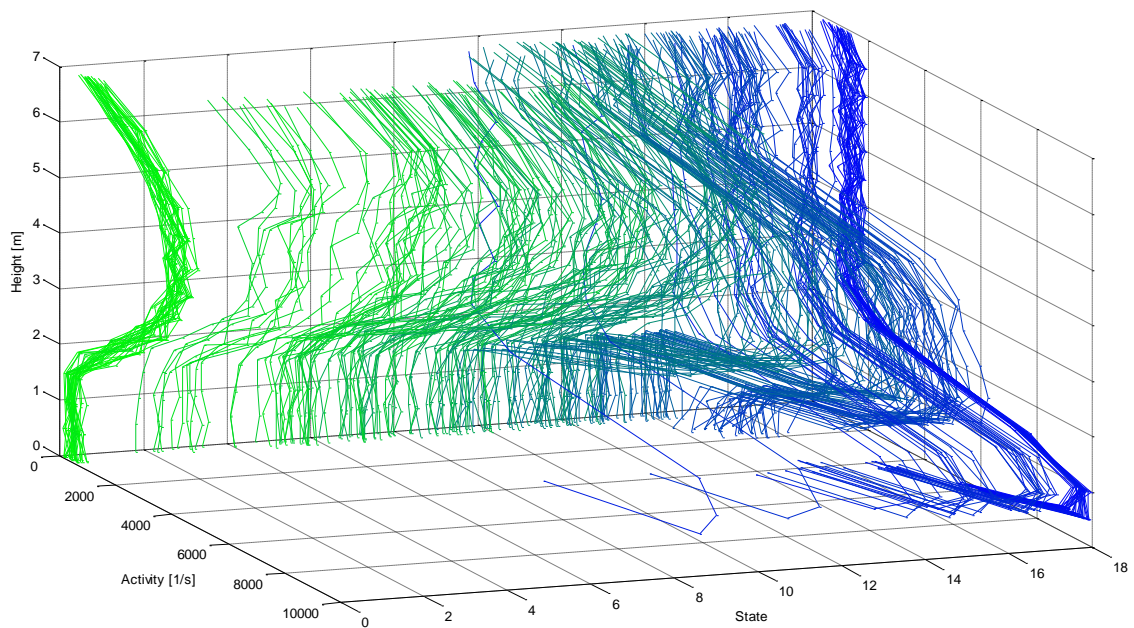


Figure 4-14: Analysis of MLP model no. 12 based on random values (recall data 3)

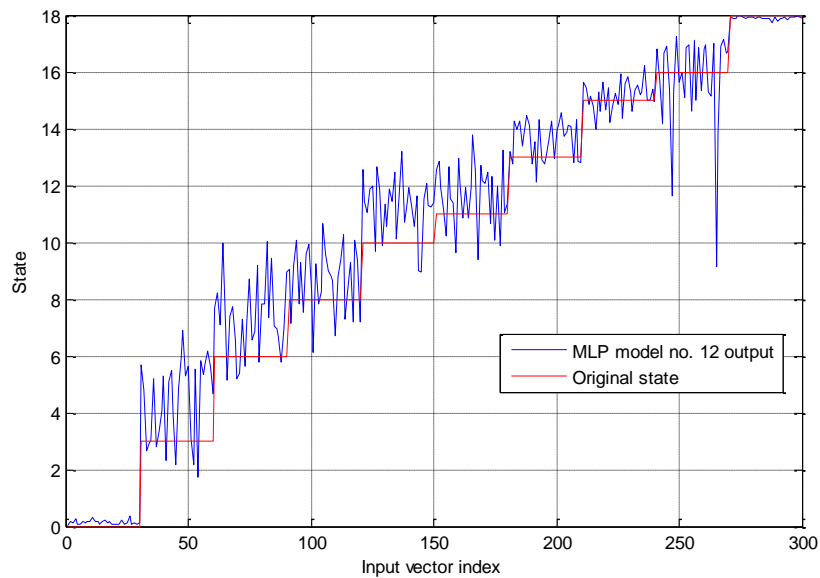


Figure 4-15: Comparison of MLP model no. 12 outputs and original states used for generation of random values

Summary

Out of 20 MLP models, two best-choice models were chosen – one with 1 HL (MLP 7), the other with 2 HLs (MLP 12). The final verification by use of random values produced based on actual values of the inputs in individual states shows that both of them are capable of correct classification of such ‘random’ input vectors. The deviation of model outputs from the original

states is, in general, smaller in case of 2HL model which thus can be considered higher-quality model. However, the desired state of such randomly generated input vectors is not known and therefore this statement is questionable.

4.5 Development of TSK models

As it was outlined above (sect. 4), two kinds of TSK models are to be developed: (1) models trained using original, not normalized data – TSK n.n., and (2) model trained using normalized data – TSK n. In some applications, normalization of the data before model training significantly improves the correctness of the model. The results of TSK n. models are thus to be compared with those of TSK n.n., and the suitability of normalization for this particular project will be assessed.

Algorithm [17] was used for the development. The first step of the model creation is determination of premise part of the fuzzy rules, i.e. finding of cluster centers based on training data and variable parameter σ (the width of Gaussian functions). After that the consequence (conclusion) part is calculated, i.e. coefficients b_{0c_i} and $b_{x_jc_i}$ are determined (see eq. (2-5)).

Since there are 10 input-output vectors in the training dataset, the maximum number of cluster (for low σ) is 10. With increasing parameter σ , the number of clusters decreases. Nine models of each kind with different numbers of clusters – from 2 to 10 – were trained.

4.5.1 TSK models by not normalized data

The above discussed width of Gaussian functions representing the clusters σ is the only variable parameter influencing the resulting model. It was observed that the internal parameters of models, trained with different σ but resulting in the same number of cluster, are identical. Thus nine models with all possible numbers of clusters were trained. The test errors are based on values stated in table 4-13 Table 4-13.

model no.	sigma	no. of cl.	max. tr. err.	mean tr. err.	max. te. err.	mean te. err.
1	4000	2	9.95E-14	5.88E-14	14.09	4.73
2	3200	3	1.95E-14	9.19E-15	1.16	0.48
3	3000	4	2.22E-14	1.24E-14	16.44	6.95
4	2000	5	1.02E-14	3.93E-15	14.38	4.60
5	1000	6	2.66E-15	8.43E-16	1.18	0.50
6	900	7	1.07E-14	4.84E-15	1.01	0.49
7	800	8	1.07E-14	3.37E-15	0.93	0.39
8	500	9	1.07E-14	4.57E-15	1.81	0.63
9	100	10	1.07E-14	4.68E-15	0.67	0.33

Table 4-12: Overview of TSK models trained using not normalized data and their respective errors

Input index	Output of model number									Desired output
	1	2	3	4	5	6	7	8	9	
1	-1.48	-0.16	-0.93	-0.53	0.50	0.54	0.55	0.54	0.54	1.00
2	5.57	2.42	0.89	1.37	1.70	1.73	1.75	1.77	1.87	2.00
3	1.64	3.55	3.45	3.42	3.58	3.63	3.61	3.51	3.43	4.00
4	5.99	4.26	4.54	4.77	4.56	4.80	4.76	4.62	4.33	5.00
5	7.00	7.00	6.90	6.95	6.90	6.85	6.86	5.19	6.97	7.00
6	9.00	8.97	8.49	8.63	8.43	7.99	8.07	9.15	8.86	9.00
7	12.00	12.02	28.44	11.65	11.97	11.97	11.96	11.99	12.09	12.00
8	14.00	14.00	9.31	13.02	13.69	13.63	13.63	13.71	13.73	14.00
9	2.91	17.00	3.39	2.62	15.82	16.14	16.99	16.99	16.99	17.00

Table 4-13: Outputs of TSK n.n. models for test input vectors and their comparison with desired outputs. The outputs whose errors exceed allowed bounds are marked red

Even though the training errors of all models are in range of round-off error, practically zero, the test errors are greater than allowed for most of the models. The same criteria used for test error evaluations of FM and MLP models apply here; the red-marked outputs do not fulfill these requirements. There are only two TSK n.n. models whose error characteristics allow for further investigations – models no. 7 and 9.

4.5.1.1 Correlation analysis of TSK n.n. models

A correlation analysis was performed by calculation of TSK-correlation coefficients K_{xy} (eq. (3-10)) and their comparison with empirical correlation factors r_{xy} .

<i>i</i>	TSK-correlation coeff. K_i of model no.									Corr. f. r_i
	1	2	3	4	5	6	7	8	9	
1	-0.03	-0.05	-0.05	-0.11	-0.29	-0.29	-0.35	-0.31	-0.51	-0.49
2	0.47	0.24	0.40	0.54	0.47	0.42	0.43	0.40	0.41	-0.52
3	-0.39	0.51	0.43	0.06	0.63	0.63	0.63	0.52	0.44	-0.59
4	-0.25	-0.51	-0.03	-0.22	-0.10	-0.18	-0.19	-0.36	-0.34	-0.57
5	0.20	0.17	0.29	0.09	0.06	0.06	0.03	-0.15	-0.22	-0.40
6	0.37	0.40	0.34	0.22	0.17	0.21	0.21	0.14	0.07	-0.12
7	-0.15	0.10	-0.07	-0.26	0.06	0.09	0.09	0.12	0.11	-0.02
8	-0.22	-0.14	-0.39	-0.52	-0.07	-0.05	-0.05	0.10	0.17	0.07
9	0.18	-0.12	-0.37	-0.29	-0.10	-0.08	-0.08	0.13	0.22	0.18
10	0.03	-0.29	-0.30	-0.06	-0.11	-0.14	-0.14	-0.01	0.05	0.32
11	-0.42	-0.30	-0.13	0.07	0.01	-0.05	-0.04	-0.03	-0.06	0.57
12	0.29	0.06	0.05	0.25	0.02	0.03	0.14	0.15	0.13	0.75
13	0.06	0.05	-0.01	0.03	0.15	0.16	0.18	0.22	0.15	0.70
14	0.07	0.06	0.05	0.08	0.23	0.24	0.22	0.26	0.18	0.69
15	0.13	0.08	0.21	0.30	0.37	0.38	0.28	0.33	0.22	0.71
sum of errors:	7.04	8.14	8.98	7.66	7.21	7.17	7.02	5.98	5.92	

Table 4-14: Comparison of correlation coefficients of TSK n.n. models with empirical correlation factors

As by MLP correlation analysis, not only the sum of absolute differences between K_i and r_i is of interest. The comparison of signs is equally important as it determines the monotony of linearized relationship. Signs of corr. coefficients of models no. 1 and 9 differ from those of empirical corr. factors in the same, smallest, number. Model no. 1, however, failed the error analysis criteria and thus cannot be considered suitable. The best-choice TSK n.n. model is therefore model no. 9.

4.5.1.2 Analysis of TSK n.n. model based on random values

The random values based analysis was performed for TSK n.n. models in the same manner as it was for FM and MLP models.

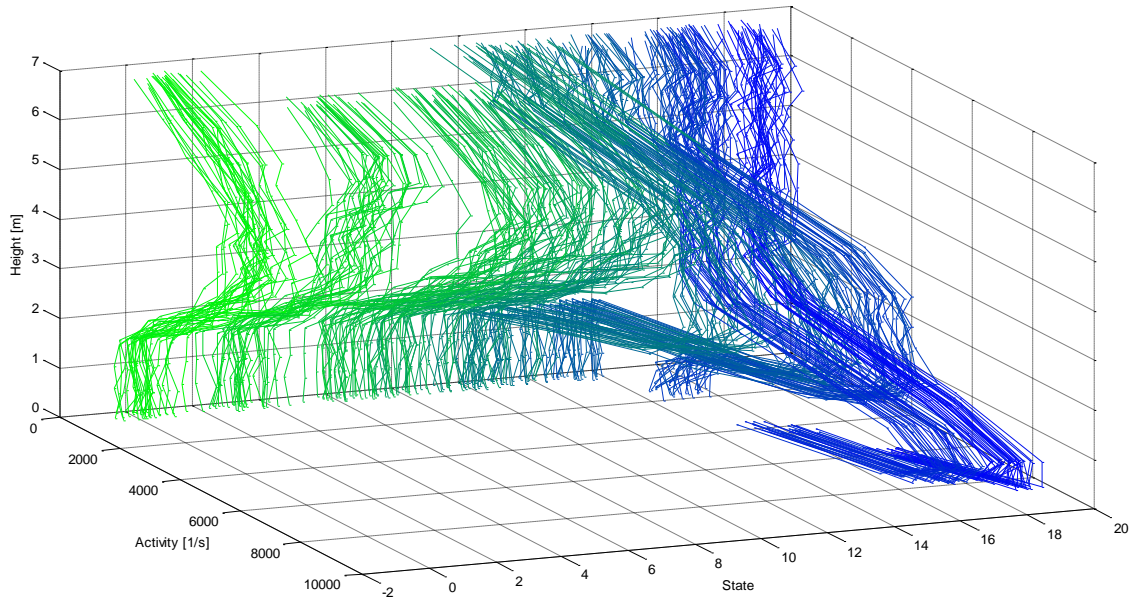


Figure 4-16: Quality analysis of TSK n.n. model no. 9 based on random values (recall dataset 3)

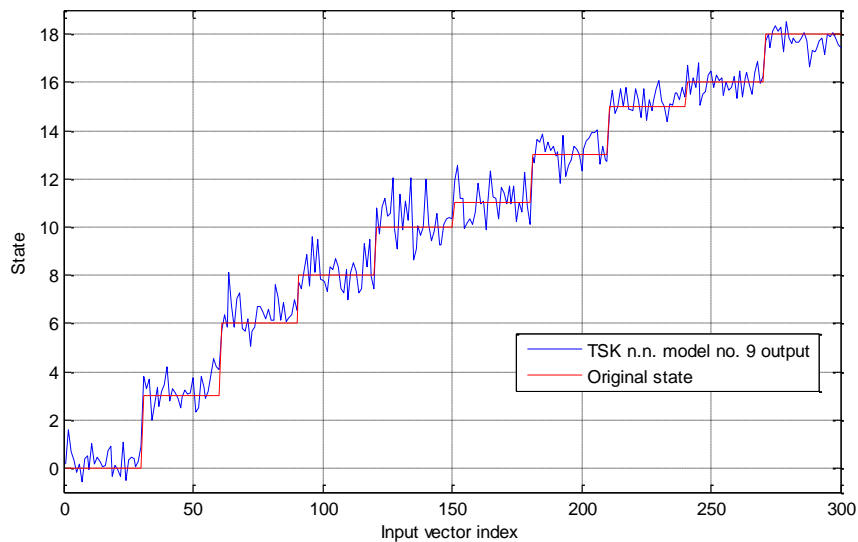


Figure 4-17: Comparison of TSK n.n. model no. 9 output for recall data and original states used for generation of the data

4.5.2 TSK models by normalized data

The development of TSK n. models was performed in the same manner as TSK n.n., with the only difference – all input-output data involved in the development process were normalized first, i.e. all input values (originally ranging from 0 to 10,000) were rescaled to the range of 0–1. Similarly, the outputs with original range 0–18 were normalized to values between 0 and 1. For better illustration and comparison with previous types of models, the model outputs were rescaled to the original range before they were evaluated.

model no.	sigma	no. of cl.	max. tr. err.	mean tr. err.	max. te. err.	mean te. err.
1	0.40	2	1.78E-14	5.76E-15	3.11	1.04
2	0.35	3	1.78E-14	1.13E-14	0.65	0.33
3	0.30	4	1.78E-14	9.73E-15	4.60	1.60
4	0.20	5	1.78E-14	9.79E-15	6.89	2.21
5	0.15	6	1.95E-14	1.16E-14	7.23	2.31
6	0.10	7	1.95E-14	1.31E-14	1.09	0.41
7	0.09	8	1.78E-14	9.90E-15	2.60	0.92
8	0.05	9	1.78E-14	5.62E-15	2.57	0.85
9	0.01	10	1.95E-14	6.18E-15	0.68	0.32

Table 4-15: Overview of TSK models trained using normalized data and their respective errors (after denormalization)

Input index	Output of model number									Desired output
	1	2	3	4	5	6	7	8	9	
1	0.84	0.36	0.43	0.87	0.79	0.61	0.54	0.55	0.56	1.00
2	2.21	2.00	1.72	2.01	2.06	1.74	1.75	1.75	1.90	2.00
3	3.49	3.49	3.43	3.36	3.57	3.71	3.56	3.56	3.44	4.00
4	4.10	4.35	4.37	4.27	4.45	4.91	4.77	4.76	4.32	5.00
5	7.00	7.00	6.95	6.94	6.93	6.83	4.40	4.43	6.98	7.00
6	9.00	8.99	8.76	8.66	8.38	7.91	9.29	9.28	8.87	9.00
7	12.00	12.00	10.27	11.95	11.93	11.96	12.03	12.02	12.17	12.00
8	14.00	14.00	14.52	13.77	13.66	13.70	13.78	13.77	13.83	14.00
9	20.11	17.00	21.60	23.89	24.23	16.81	18.06	16.99	16.99	17.00

Table 4-16: Rescaled outputs of TSK n. models for test input vectors and their comparison with desired outputs. The outputs whose errors exceed allowed bounds are marked red

Similar error characteristics with TSK n.n. models may be observed with the TSK n. models – negligible training errors and larger test errors which exclude most of the models from further investigations. The only models that were capable of correct classification of all test input vectors are models no. 2 (3 clusters) and no. 9 (10 clusters).

4.5.2.1 Correlation analysis of TSK n. models

The same quality analysis as for TSK n.n. models was performed for the TSK n. models – the correlation analysis, and random numbers based analysis.

<i>i</i>	TSK-correlation coeff. K_i of model no.									Corr. f. r_i
	1	2	3	4	5	6	7	8	9	
1	-0.12	-0.10	-0.09	-0.10	-0.07	-0.21	-0.15	-0.20	-0.42	-0.49
2	0.14	0.43	0.55	0.51	0.39	0.39	0.35	0.36	0.40	-0.52
3	0.42	0.53	0.52	0.50	0.49	0.65	0.53	0.55	0.47	-0.59
4	-0.19	-0.24	0.13	0.12	0.04	-0.12	-0.36	-0.38	-0.33	-0.57
5	-0.13	0.06	0.25	0.25	0.28	0.15	-0.08	-0.09	-0.18	-0.40
6	0.31	0.29	0.25	0.27	0.38	0.31	0.19	0.22	0.11	-0.12
7	0.34	0.29	0.18	0.19	0.26	0.20	0.20	0.23	0.19	-0.02
8	0.38	0.29	0.12	0.11	0.14	0.06	0.18	0.21	0.27	0.07
9	0.32	0.31	0.14	0.12	0.13	0.01	0.18	0.22	0.31	0.18
10	-0.11	0.16	0.12	0.12	0.09	-0.08	0.01	0.04	0.11	0.32
11	-0.37	0.05	0.11	0.14	0.11	-0.01	-0.04	-0.02	-0.03	0.57
12	0.15	0.05	0.08	0.12	0.15	-0.02	-0.04	0.07	0.07	0.75
13	0.16	0.11	0.21	0.23	0.24	0.12	0.16	0.16	0.10	0.70
14	0.18	0.15	0.25	0.27	0.28	0.21	0.26	0.22	0.13	0.69
15	0.22	0.20	0.28	0.31	0.31	0.37	0.43	0.31	0.18	0.71
sum of errors:	7.44	7.34	7.29	7.11	7.17	7.42	6.44	6.55	6.48	

Table 4-17: Comparison of correlation coefficients of TSK n. models with empirical correlation factors

As for the sign comparison, models no. 2, 8 and 9 differ in the smallest number, 5. Model no. 8, however, did not fulfill the test error criteria. The comparison of values shows significantly better concurrence of model no. 9 coefficients and therefore this model can be considered the best-choice TSK n. model.

4.5.2.2 Analysis of TSK n. model based on random values

The best-choice TSK n. model, according to analysis from previous section, model no. 9 was further investigated using the random values from recall dataset no. 3.

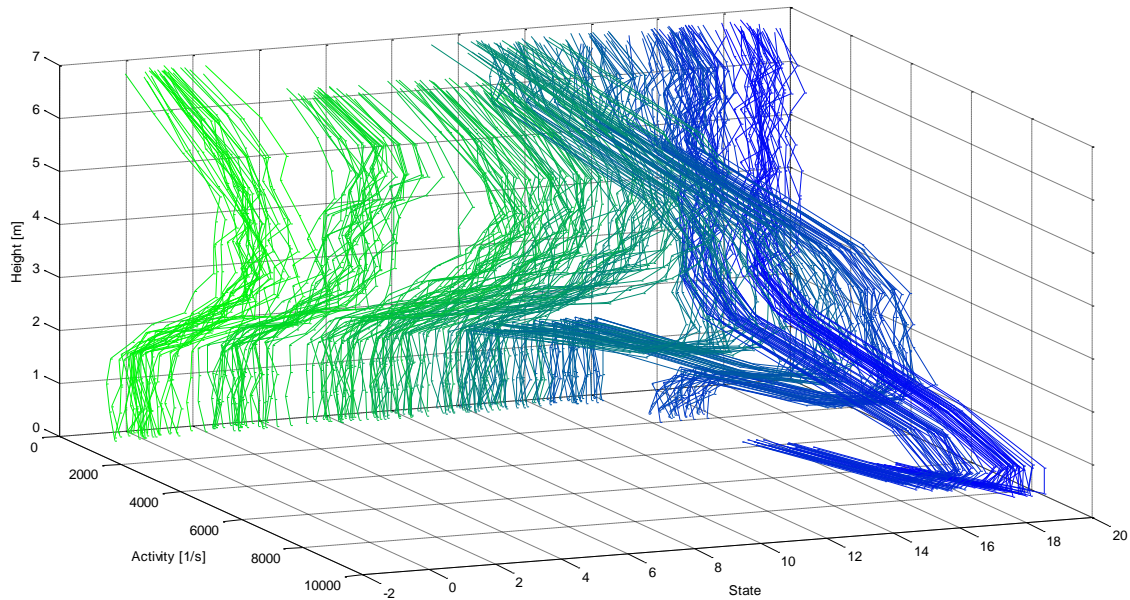


Figure 4-18: Quality analysis of TSK n. model no. 9 based on random values (recall dataset 3). Both input and output data were denormalized for better illustrativeness

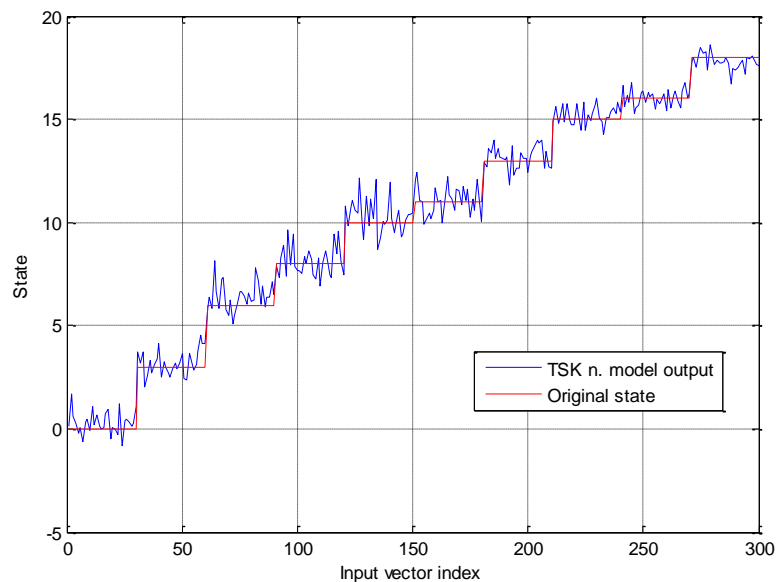


Figure 4-19: Comparison of denormalized TSK n. model no. 9 outputs for recall data and original states used for generation of the data

4.6 Comparison of models

All of the trained models passed the training errors criteria. In case of TSK models, the training errors are in range of round-off error. The tr. errors of FM model are negligible in most cases. Higher values for the first and the last data pattern are caused by the COG defuzzification method. The range of output variable is set to 0–18 and thus the parts of membership functions exceeding these limits are not taken into account. The training errors of MLP models are notably greater but all manage to classify the input vectors correctly.

The fuzzy model by Mamdani exhibits also the lowest test errors, even though as it was mentioned before (4.2), there is no guarantee that lower test error signifies better model in this particular application. The test error criteria were what most of the TSK models failed and the best-choice models selection was made mostly by this evaluation. Right on contrary, none of the MLPs was dismissed based on test errors as they all satisfied the requirements.

The outputs of the best-choice models for the recall dataset no. 3 are provided on figure 4-20. For better illustrativeness, the original states, i.e. the states whose input values were used for generation of random vectors, were subtracted from the model-outputs and these ‘errors’ are plotted.

There is a region (between input index 60 and 120) in case of FM model, where the original and model outputs differ largely. For the rest of the input vectors, the differences are low and practically zero. None of these phenomena is desired. Even though the model output should correspond to the original state, the random vectors differ from the original ones and so should the output, despite the fact that the desired state is not defined for the random vectors and thus the exact error cannot be calculated.

The results for MLP and TSK models show similar behavior with notably lower oscillations around the original state in case of TSK models. These characteristics imply slightly better suitability of TSK models for core state diagnosis. Since the maximum deviation of individual random vectors’ elements is as low as 500 imp/s, the large differences of model outputs from the original states (as by MLPs – in some cases greater than 4) are not expected. The ‘errors’ of TSK models are observable and thus the effect of random vectors is apparent but they are small enough so that the original state is clearly identifiable.

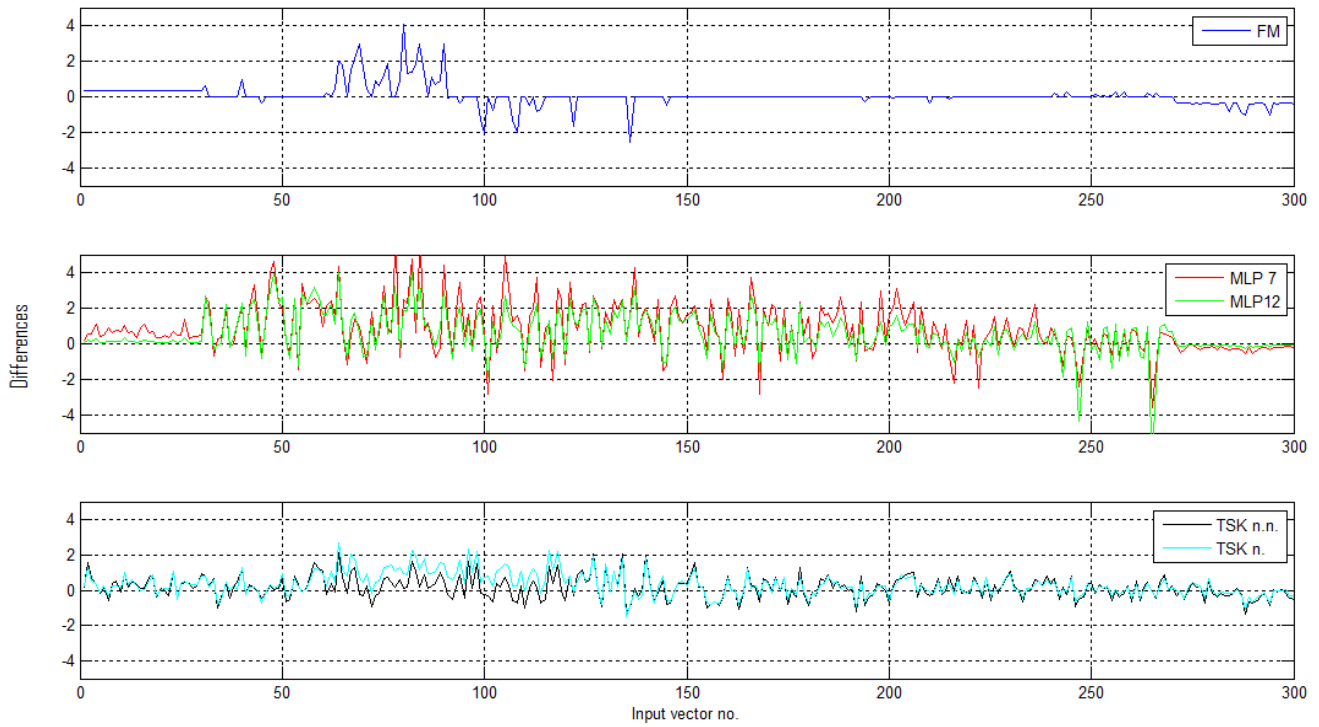


Figure 4-20: Comparison of outputs of the best-choice models for the recall dataset no. 3 (after subtraction of original states)

5 Sensitivity analysis of the models

5.1 General method of sensitivity analysis

In this chapter, the sensitivity of the best-choice models is to be analyzed. The sensitivity is measured as a change of model outputs in case of sensors (inputs) malfunction. Two different types of sensors failures are assumed:

- sensor with zero output (zero failure), and
- sensor with random output (random failure).

Furthermore, after analysis with one malfunctioning sensor is conducted, the behavior of the models in case of failure of two sensors is to be performed. Since there are 15 inputs for each model and thus the total number of all possible pairs of sensors is too large, only pairs of adjacent inputs are taken into account.

The recall dataset no. 3 was used for the analysis. In the first case the vectors of individual inputs were replaced by zeros, one at a time, and outputs of all the models were calculated for such new 15 datasets. Then the procedure was repeated, this time with two adjacent inputs, generating 14 new datasets for which the model outputs were calculated.

The production of datasets for the second assumed sensor failure – sensors producing random values – was analogous, only the input vectors were not replaced by zeros but with random values generated with respect to range of values of the inputs in the training dataset. The interval of the training data values was extended by ca. ± 500 –1000 as seen in table 5-1 Table 5-1:

Input no.	Range of values	Input no.	Range of values	Input no.	Range of values
1	0–5000	6	500–9000	11	500–9500
2	500–6000	7	500–9000	12	500–11000
3	500–7000	8	500–9500	13	500–11000
4	500–7000	9	500–9500	14	500–11000
5	500–8000	10	500–9500	15	500–7000

Table 5-1: Range of random values used for data generation in sensitivity analysis

There is a total of 58 different input datasets (2 x 15 with single- + 2 x 14 with double input failure) for which the models are tested. Multiplied with 5 models, it provides a total of 290 different outputs to be analyzed. Only the most important and significant of them are stated in following chapters in order to maintain a good illustrativeness of this work.

5.2 Results of sensitivity analysis using zero inputs

New datasets produced with use of recall data no. 3 by means described in previous chapter for the first assumed sensor failure (zeros) were taken as inputs for all best-choice models. The respective outputs were then compared with outputs of the model obtained for original recall dataset no. 3 and sum of differences was calculated.

Failure of input no.	FM	MLP 7	MLP12	TSK n.n.	TSK n.
1	1390	121	184	287	224
2	516	1674	1560	745	763
3	562	697	185	863	946
4	1280	999	410	294	340
5	632	1397	627	157	183
6	1390	194	124	395	414
7	1390	125	288	382	498
8	1390	141	781	393	559
9	1390	931	921	426	557
10	1390	1296	860	101	153
11	1390	786	270	65	121
12	646	102	103	233	238
13	644	310	331	390	422
14	640	512	636	416	453
15	644	1116	1206	278	331
Average:	1020	693	566	362	413

Table 5-2: Sums of differences of model outputs caused by zero failure of single inputs (maximum values marked red, minimum values marked green)

Failure of inputs no.	FM	MLP 7	MLP12	TSK n.n.	TSK n.
1+2	1390	1632	1513	467	494
2+3	564	1452	1517	1534	1592
3+4	1323	388	289	595	573
4+5	1390	1781	1044	453	562
5+6	1390	1255	789	432	353
6+7	1390	309	439	761	858
7+8	1390	16	1256	783	1032
8+9	1390	1081	1830	850	1122
9+10	1390	1840	1899	568	738
10+11	1390	1748	1453	137	141
11+12	1390	623	197	263	242
12+13	646	129	65	653	671
13+14	640	977	998	716	777
14+15	640	1426	1294	631	665
Average:	1166	1047	1042	632	701

Table 5-3: Sums of differences of model outputs caused by zero failure of two adjacent inputs (maximum values marked red, minimum values marked green)

Discussions of partial results for each model are provided in following subsections.

5.2.1 Fuzzy model by Mamdani

The general quality of the FM model in terms of sensitivity was expected to be the worst of all the models. The quality analysis based on random values has shown that the FM model is very good as for classification of vectors close to those defined in training dataset but once at least one input exceeds the defined range, the situation that no rule is valid occurs and the output of the model is 9 (see sect. 0).

The FM model is capable to classify correctly only those input vectors referring to broken sensors 12–15 and lower states (where these inputs are 0 by definition), and on the contrary, broken sensors 2, 3, and partially 4 and 5 in higher states where these inputs are generally low.

The analysis of results with double input failure show similar behavior of the model for sensors 12–15 and low states, and sensors 2 and 3 in high states. The failure of any other pair of sensors leads to output 9 for all of the input vectors.

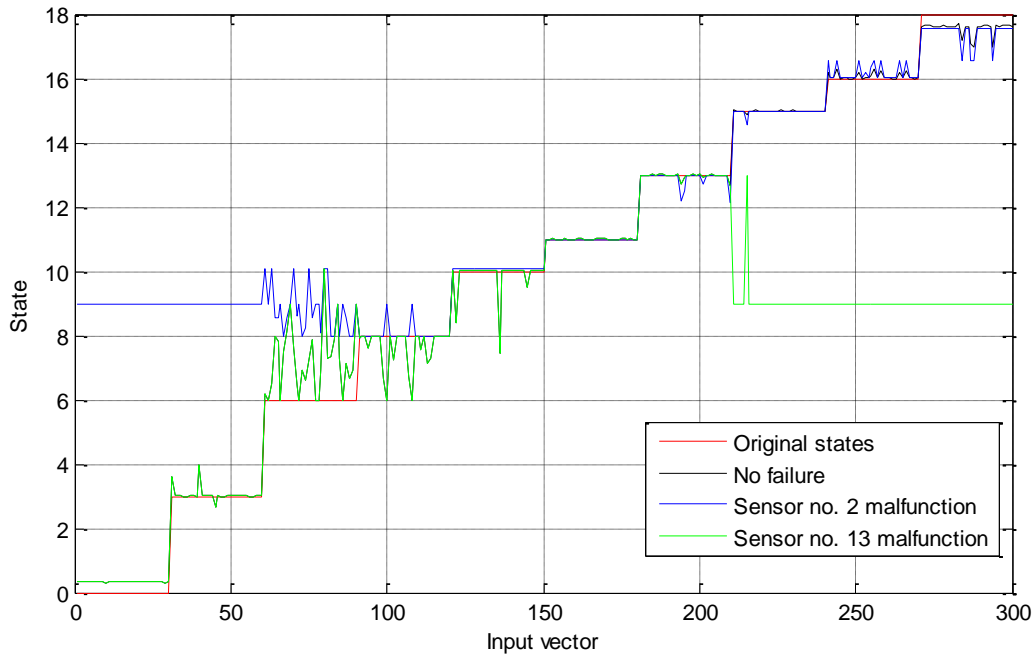


Figure 5-1: Comparison of original states used for data generation (red), output of FM models (black), output of FM model with zero input no. 2 (blue), and output of FM model with zero input no. 13 (green). The black and green lines overlap perfectly until input vector no. 210

5.2.2 MLP models

The overall sensitivity of MLP models with respect to that of FM model is expected to be lower. While the FM model returns meaningless output for inputs out of the ranges defined in the rule base, the MLP calculates unique output for every possible combination of inputs.

Following findings were obtained by sensitivity analysis of MLP model no. 7 (1 hidden layer) for a single input malfunction:

- model is rather insensitive to failure of inputs no. 1, 7, 8 and 12,
- the largest change of outputs is caused by failure of inputs no. 2, 5, 10 and 15.

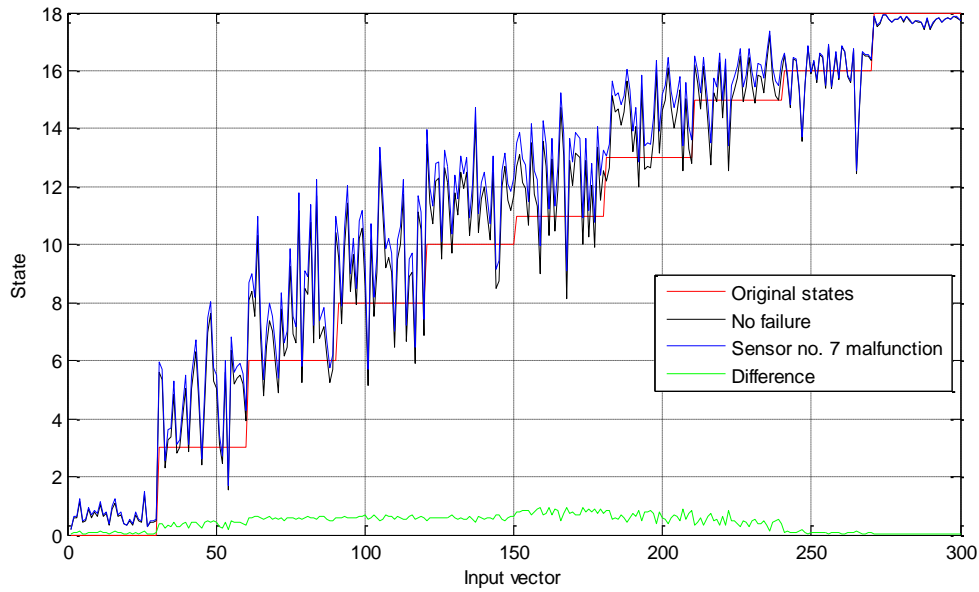


Figure 5-2: Sensitivity analysis of MLP model no. 7: original states used for data generation (red), original MLP model output (black), output of MLP model with zero input no. 7, and the difference between these two outputs (green)

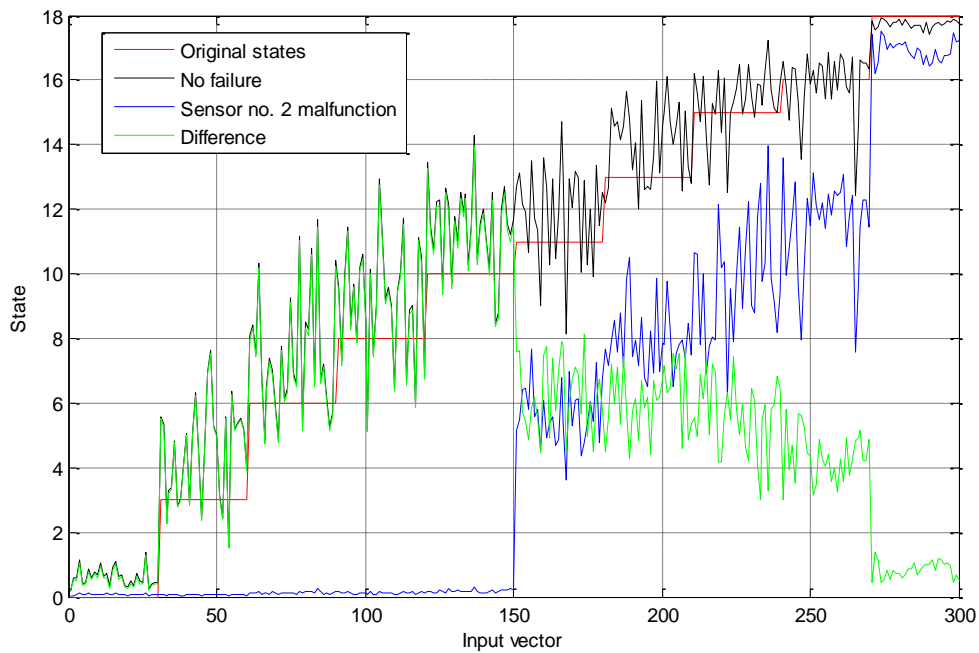


Figure 5-3: Sensitivity analysis of MLP model no. 7: original states used for data generation (red), original model output (black), output of the model with zero input no. 2, and the difference between these two outputs (green)

One can observe that although the failure of input no. 7 does not influence the model outputs in a significant way, the input no. 2 malfunction completely devalues the classification. Also is not out of interest that the sensitivity to individual inputs failures somehow corresponds with

correlation weights of the model (table 4-9Table 4-9). The inputs with low sensitivity listed above introduce, in general, lower correlation weights, and vice versa.

For a double input failure, the differences in model outputs are generally larger. Also it is observed that failure of two inputs with higher individual sensitivities results in higher differences of the outputs and vice versa.

As for the 2HL best-choice MLP (model no. 12), a significant correlation of the sensitivities of individual input failures with respect to model no. 7 can be noticed. The lowest sensitivity is recorded for failure of single inputs no. 1, 3, 6 and 12, and for combination of failures of inputs no. 3 + 4, 11 + 12, and 12 + 13. In contrast, the highest sensitivity is experienced for single failures of inputs no. 2, 9, 10 and 15, and for all combinations containing any of these. Also these findings correspond with absolute values of correlation weights of the model (table 4-10Table 4-10).

5.2.3 TSK models

Sensitivity of the TSK models explored by use of zero inputs is generally the lowest of all models. Taking sum of differences between outputs of models without and with input failure as a measure of sensitivity, the maximum as well as average value of it in case of TSK models is lower compared to those of the other models (see Table 5-2table 5-2 and table 5-3).

Also significant correlation of values from cited tables belonging to TSK models is observed (correlation factor of ca. 0.97 in both cases). Both models (TSK n.n. and TSK n.) exhibit the lowest sensitivity in case of failure of single inputs no. 5, 10 and 11; the highest sensitivity is then experienced for inputs no. 2 and 3. Somewhat relation of the sensitivity to the TSK correlation coefficients (table 4-14Table 4-14, table 4-17) can be found, although not as strong as in case of MLP corr. weights.

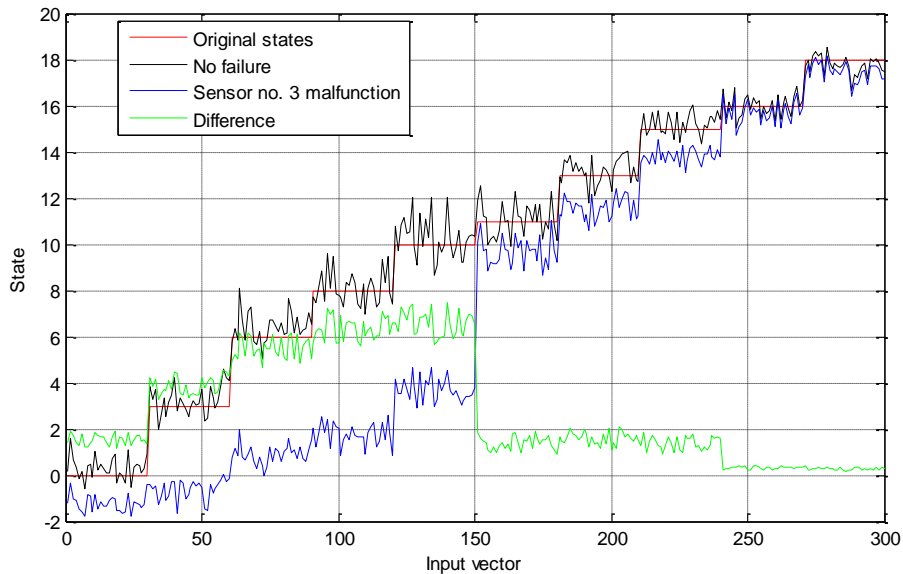


Figure 5-4: Sensitivity analysis of TSK n.n. model no. 9: original states used for data generation (red), original model output (black), output of the model with zero input no. 3, and the difference between these two outputs (green)

5.3 Results of sensitivity analysis using random inputs

Next, a similar analysis has been performed with the zero inputs been replaced by random values. The previously assumed failure of the sensors (zero outputs) is reasonably easy to be diagnosed. The behavior of the models in case of more treacherous failure – random output – is studied in this section as this kind of malfunction is more difficult to be recognized and subsequently rectified, especially when the range of values is not conspicuously far from the expected ones (those defined in the training dataset). The range of random values for individual inputs is stated in table 5-1Table 5-1.

The results were analyzed in the same manner as those from sect. 5.2, i.e. by calculation of sums of differences in outputs caused by respective failure of a single input or a pair of inputs.

Failure of input no.	FM	MLP 7	MLP12	TSK n.n.	TSK n.
1	515	103	201	211	206
2	288	971	830	500	531
3	376	498	125	702	765
4	594	490	175	103	137
5	409	672	275	120	144
6	785	81	51	290	288
7	903	62	137	320	358
8	906	72	354	387	449
9	979	512	451	442	480
10	1038	915	520	303	310
11	922	717	282	186	194
12	982	475	410	710	521
13	723	823	597	753	606
14	896	1138	1039	791	655
15	890	1663	1764	453	395

Average:	747	613	481	418	420
-----------------	-----	-----	-----	-----	-----

Table 5-4: Sums of differences of model outputs caused by random failure of single inputs (maximum values marked red, minimum values marked green)

Failure of inputs no.	FM	MLP 7	MLP12	TSK n.n.	TSK n.
1+2	687	971	837	502	522
2+3	479	925	811	1109	1160
3+4	792	512	185	689	728
4+5	814	898	397	180	192
5+6	964	653	298	345	324
6+7	1166	113	156	481	487
7+8	1204	76	420	610	664
8+9	1258	546	682	740	796
9+10	1283	1254	911	702	716
10+11	1259	1375	704	449	433
11+12	1208	643	342	829	642
12+13	1181	577	400	1272	1047
13+14	1034	1697	1546	1416	1233
14+15	1141	2174	2297	1181	1024

Average:	1033	887	713	750	712
-----------------	------	-----	-----	-----	-----

Table 5-5: Sums of differences of model outputs caused by random failure of two adjacent inputs (maximum values marked red, minimum values marked green)

5.3.1 Fuzzy model by Mamdani

As it was mentioned previously, the behavior of the FM model is treacherous. There are a lot of cases that the model is not able to classify the input vector when working with random numbers. For reasons stated in sect. 0, this results in model output equal to 9. Most of the sensitivity analysis graphs of FM model in case of single input random failure are thus similar as shown on figure 5-5.

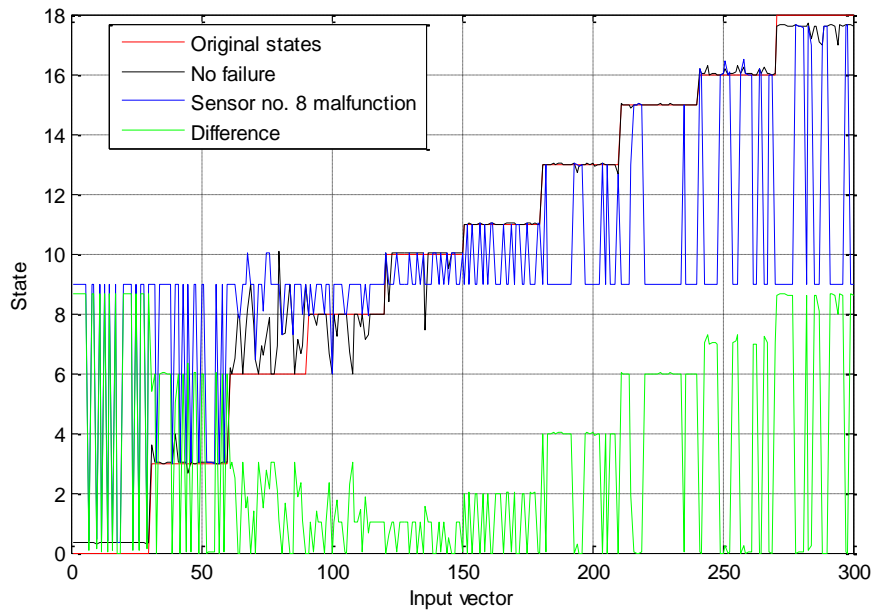


Figure 5-5: Sensitivity analysis graph of FM model – random failure of input no. 8: original states used for data generation (red), original model output (black), output of the model with random input no. 8, and the difference between these two outputs (green)

The behavior is similar in case of random failure of two inputs. The share of unclassified inputs is generally higher compared to failures of single inputs, which is represented by longer uninterrupted segments of straight blue line at state 9 in figure 5-6.

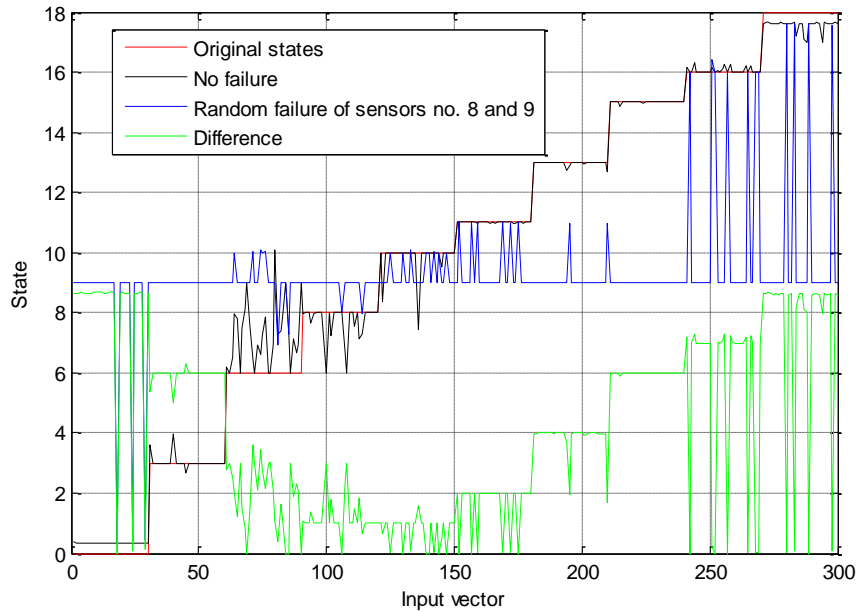


Figure 5-6: Sensitivity analysis graph of FM model – random failure of inputs no. 8 and 9: original states used for data generation (red), original model output (black), output of the model with random inputs no. 8 and 9, and the difference between these two outputs (green)

5.3.2 MLP models

The results of sensitivity analysis for random failures are comparable in cases of both MLP models, with slightly better results for MLP 12 (model with 2 HLs). Also the expected outcome, i.e. significant correlation with zero failure analyses, was confirmed.

While random failure of some inputs (no. 1, 6, 7 and 8 for MLP 7, and no. 3, 6 and 7 for MLP 12) cause rather negligible changes of model outputs, failure of others, such as no. 2, 5, 10, 11, 13, 14 and 15 (MLP 7), resp. no. 2, 13, 14 and 15 (MLP 12), results in serious differences, making it impossible to correctly classify the original state. The high sensitivity of MLP models on sensors no. 13, 14 and 15 is given by the training data set. Activity is not registered in the lower region until the very late states, and thus the application of random values for these inputs results in greater outputs of the model, as seen on figure 5-7.

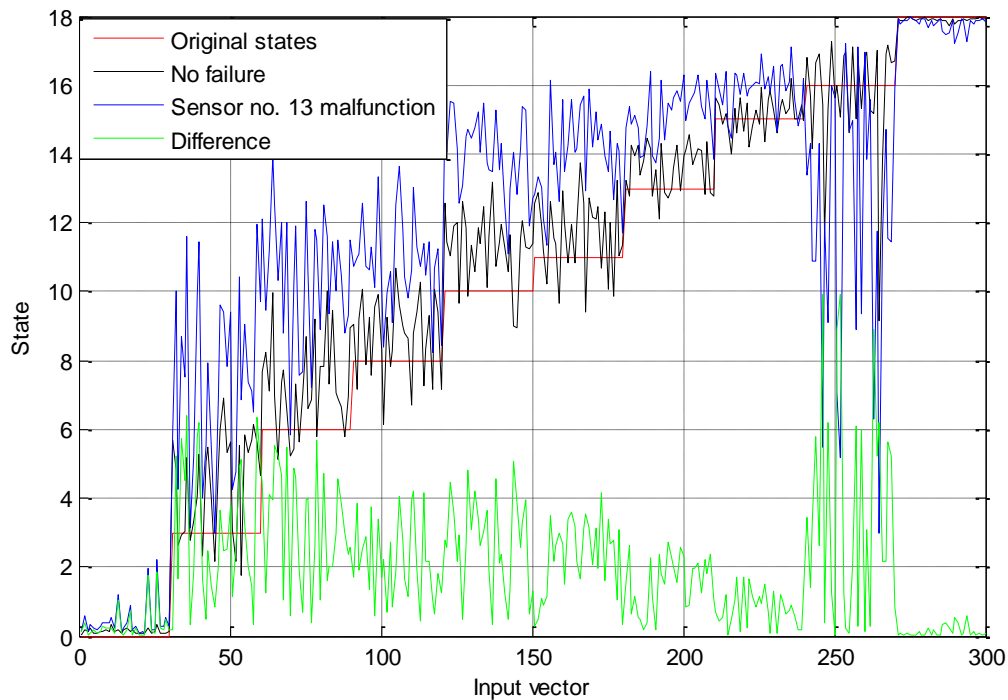


Figure 5-7: Sensitivity analysis graph of MLP model no. 12 – random failure of input no. 13: original states used for data generation (red), original model output (black), output of the model with random input no. 13, and the difference between these two outputs (green)

This phenomenon may also provide an answer to behavior of the MLP models observed previously. Figures 4-13 and 4-15 show comparison of MLP outputs for original recall dataset no. 3 and the states used for its generation. One can observe that the mean value of the outputs for each section of 30 inputs lies above the red line (original states), until state 15. This is most likely caused by the random values introduced in the last three inputs, since as it was proven in this section that these inputs considerably increase the lower states. This finding also corresponds with the high, positive correlation weights.

5.3.3 TSK models

Both TSK models act in an extremely similar way – the correlation factor of sums of errors for single random failure (table 5-4Table 5-4) is 0.91, and for double random failure (table 5-5Table 5-5) is 0.97. The random failure analysis confirmed the good results of the TSK models obtained in sect. 5.2.3. An opposite trend was observed by the TSK models: While the FM and MLP models exhibit smaller change of outputs in case of random failure than for the zero failure, the TSKs are more influenced by the random failures.

The TSK models are mutually the most sensitive to random failures of inputs no. 2, 3, 12, 13 and 14 while the failure of inputs no. 4, 5 and 11 causes relatively small change of outputs. The TSKs appear to have the lowest sensitivity for failure of those inputs which have negative correlation coefficient (table 4-14, table 4-17) and also the high sensitivity to inputs no. 2 and 3 can be foreseen by high positive respective correlation coefficients, but there is no concurrence which would make it possible to estimate the sensitivity to some input based on corr. coefficients.

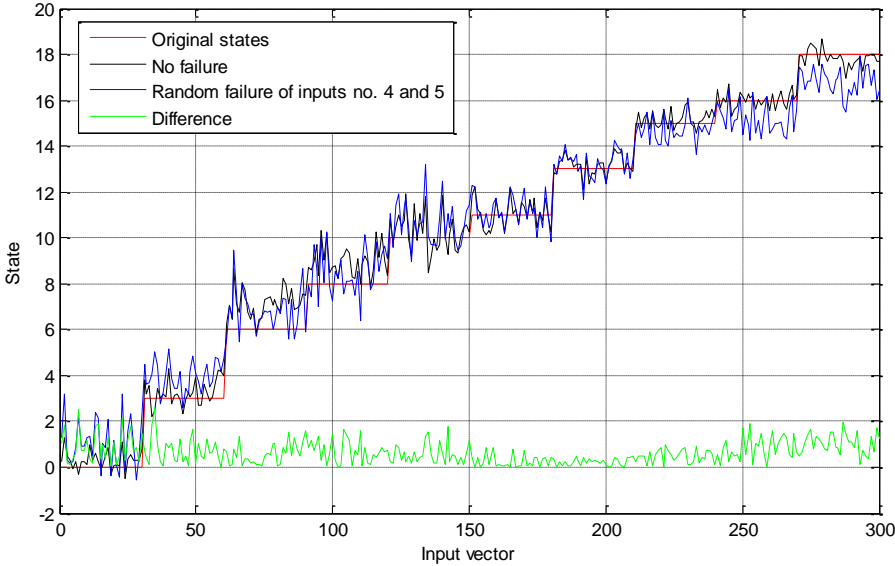


Figure 5-8: Sensitivity analysis graph of TSK n. model no. 9 – random failure of inputs no. 4 and 5: original states used for data generation (red), original model output (black), output of the model with random inputs no. 4 and 5, and the difference between these two outputs (green)

5.4 Summary of sensitivity analysis results

There are large differences in behavior of the individual models in terms of their sensitivity to zero failures of inputs. The FM model appeared to be the most sensitive as the failure of mostly any input is crucial for the core state classification. A high degree of correlation of sensitivities was recorded for the pairs of models of the same type (MLPs and TSKs). The TSK models exhibit in general the lowest sensitivity; slightly better results are obtained in case of model trained using not normalized data (TSK n.n.).

One of the most important findings is that there is a large consensus between correlation weights of the MLPs and the experienced sensitivity. There are also some similarities in case of the corr.

coefficients of the TSKs and their sensitivity characteristics but a general trend cannot be concluded.

5.5 Recommendations based on sensitivity analysis

The sensitivity analyses have shown that there are a lot of cases when a failure of an input causes a total misinterpretation of the original core state. The best prevention is a monitoring of all sensors and a prompt replacement of the malfunctioning ones, yet there can be some measures taken in order to enhance the core state classification in case of a sensor failure.

An interesting phenomenon is observed for some failures of MLPs. In a few cases, the combined sensitivity to a zero failure of two adjacent inputs is lower than individual sensitivities to a single zero failure of any of those inputs. For instance, a single zero failures of inputs no. 3 and 4 result in a total sum of errors of 697 and 999 respectively but a coincident failure of both these inputs gives a sum of errors 388. A table of inputs with such behavior could be produced and in case of failure of any of those, the second input would be dismissed in order to lower the sensitivity.

This measure however applies only to the MLP models and only in several special cases. A more general approach is to recover the missing input by use of other input values. The most suitable method for the data recovery would be a subject of further investigations.

6 Conclusion

The main task of this thesis was the development of SC models using appropriate simulation tools for the classification of core states during a nuclear meltdown. There are a total of 5 best-choice models of different types: fuzzy model by Mamdani, MLP model with 1 HL, MLP model with 2 HLs, TSK model trained by not normalized data and TSK model trained by normalized data. In order to create these models, datasets for their development and subsequent quality analyses had to be generated first. Postulated gamma distribution of individual states of core meltdown was used for the data generation.

There were a total of 20 MLP models trained with different architectures (different number of neurons in hidden layers and different transfer functions) – 10 with 1 hidden layer and 10 with 2 HLs. Since there are only 10 data patterns in the training dataset, the maximum number of clusters of the TSK models with cluster algorithm by Wong and Chen is 10. There were nine models trained with different numbers of clusters (from 2 to 10) of each type – TSK n.n. and TSK n. Out of these models, the best-choice ones of each type were selected according the performed quality analysis.

The quality of the models was analyzed firstly by error characteristics (training- and test errors). With respect to specifics of this application, requirements for the test errors have been set. The quality analysis based on internal parameters is only applicable to MLPs and TSKs. First, the statistical properties of weight coefficients (MLP) were inspected as high absolute values of the weights or large span would imply a poor model quality. Then the weight analysis by means of comparison of correlation weights of the models with empirical correlation factors of the training input data was performed. Similarly, the TSK-correlation coefficients were calculated for all TSK models and compared with the empirical corr. factors.

The best-choice models were further analyzed based on random values (recall dataset no. 3 – 30 data patterns for each training state with random input values in range of ± 500 imp/s from the input values of the training state). Although the desired state is not known for these random vectors and thus the errors cannot be calculated, this analysis may provide an overview of important characteristics and behavior of the models.

The sensitivity analysis was performed in order to ascertain the behavior of the models, mainly the change of their outputs, in case of various failures of inputs. Two types of failures were assumed: sensor generating zero output, and sensor generating random output. The recall dataset no. 3 was altered several times to represent said failures either of one or of two adjacent

inputs, and the outputs of the best-choice models were calculated. Measure of sensitivity was defined as a sum of differences between outputs of the model for original recall dataset no. 3 and those for the dataset representing chosen sensor malfunction.

Fuzzy model by Mamdani was created by establishing of a set of rules with combination of input values from the training dataset in the antecedent and the respective number of the core state in the succedent. The quality of the model appeared to be sufficiently good as for classification of the training- and test states. The random numbers based analysis as well as the sensitivity analysis however showed some undesired behavior which does not support the use of FM model in this form as a suitable core state classification tool.

All of trained MLP models satisfied the error criteria. While all of the models passed the statistical evaluation with good results, there were large differences between the corr. weights and actual corr. factors. Two best-choice models were selected – MLP no. 7 (1 HL) and MLP no. 12 (2 HLs). The random numbers based analysis has shown slightly better results in case of MLP no. 12. The sensitivity analysis has revealed a strong relation between absolute value of correlation weights of the MLP and the sensitivity to failure of respective input.

Most of the TSK models did not fulfill the test error requirements. The correlation analysis was performed similarly to MLP models and also with similar results. The two best-choice models are those with the highest number of clusters. The random numbers based quality analysis as well as the sensitivity analysis of the TSK models showed the best results of all models. The models also appear to be the least sensitive to failures of inputs with negative correlation coefficients but the absolute value does not seem to have an influence on the sensitivity, neither for the positive, nor for the negative coefficients.

There are some suggestions provided at the end of the sensitivity analysis chapter in order to lower the effect of input failure. For several special cases, a failure of 2 inputs of MLP model causes smaller change of output than a single failure of any of these inputs. More investigations could be made to study this effect not only for adjacent inputs but also for any possible pair of inputs. Should there be more of these cases, the input numbers would be put in a table and in case of failure of any of these inputs, the associated input would be dismissed, too.

A more general measure against the input failure sensitivities is to restore the value of the broken sensor based on values of the functioning ones. A possible approach would be to create a SC model for each sensor (a fuzzy model by Mamdani might be an appropriate choice) whose inputs are the other 14 sensors and the output is the restored activity of this particular,

malfunctioning sensor. More research is required in this matter regarding the most suitable type of SCM, or behavior of such models in case of failure of two arbitrary inputs.

References

- [1] S. Schmidt, D. Fiß, E. Rudolph und A. Kratzsch, Signifikante Zustände von projektrelevanten Kernschmelzszenarien und erste Instrumentierungsvorschläge für das Verbundvorhaben "NIZUK", Technische Dokumentation, IPM, 2013.
- [2] G. Kessler, Sustainable and safe nuclear fission energy - Technology and Safety of Fast and Thermal Nuclear Reactors, Heidelberg: Springer, 2012.
- [3] World Nuclear Association, „WNA Reactor Database,“ [Online]. Available: <http://www.world-nuclear.org/nucleardatabase/Default.aspx?id=27232>. [Zugriff am 1 June 2013].
- [4] T. K. Ghosh und M. A. Prelas, Energy Resources and Systems - Volume 1: Fundamentals and Non-renewable Resources, Dordrecht: Springer, 2009.
- [5] C. R. Nave, "HyperPhysics," Georgia State University, 2013. [Online]. Available: <http://hyperphysics.phy-astr.gsu.edu/hbase/nucene/reactor.html#c3>. [Accessed 10 May 2013].
- [6] H. Kleykamp, J. O. Paschoal, R. Pejsa und F. Thommler, „Composition and Structure of Fission Products Precipitates in Irradiated Oxide Fuels,“ *Journal of Nuclear Materials*, Nr. 130, p. 426–433, 1985.
- [7] G. Brillant, C. Marchetto und W. Plumecocq, „Fission product release from nuclear fuel I. Physical modelling in the ASTEC code,“ *Annals of Nuclear Energy*, 2013.
- [8] V. Slugeň, Safety of VVER-440 Reactors - Barriers Againsts Fission Products Release, London: Springer, 2011.
- [9] P. Hoffman, „Current knowledge on core degradation phenomena, a review,“ *Journal of Nuclear Materials*, Nr. 270, pp. 194-211, 6 November 1999.

- [10] W. Hering und C. Homann, „Degraded core reflood: Present understanding,“ *Nuclear Engineering and Design*, Nr. 237, pp. 2315-2321, 22 April 2007.
- [11] W. C. Müller, „Review of debris bed cooling in the TMI-2 accident,“ *Nuclear Engineering and Design*, pp. 1965-1975, 20 March 2006.
- [12] Reinke, Nils, et al., „Formation, characterisation and cooling of debris: Scenario discussion with emphasis on TMI-2,“ *Nuclear Engineering and Design*, Nr. 236, pp. 1955-1964, 26 March 2006.
- [13] Struwe, D., et al., Consequence evaluation of in-vessel fuel coolant interactions in the European pressurized water reactors, Karlsruhe: Forschungszentrum Karlsruhe GmbH, 1999.
- [14] A. L. Wright, Primary System Fission Product Release and Transport, State-of-the-Art Report to the Committee on the Safety of Nuclear Installations, Oak Ridge: Oak Ridge National Laboratory, 1994.
- [15] L. A. Zadeh, „Fuzzy Sets,“ *Information and Control*, pp. 338-353, 30 November 1965.
- [16] H. Lutz und W. Wendt, Taschenbuch der Regelungstechnik, 7. ergänzte Auflage, Frankfurt am Mein: Wissenschaftlicher Verlag Harri Deutsch, 2007.
- [17] C.-C. Wong and C.-C. Chen, "A Clustering-Based Method for Fuzzy Modeling," *IEICE Trans. Inf. a Syst.*, Vols. E82-D, no. 6, pp. 1058-1065, june 1999.
- [18] S. Schmidt, Vergleichende Analyse von Soft Computing Verfahren zur Modellierung verfahrenstechnischer Prozesse, Masterarbeit, Hochschule Zittau/Görlitz, IPM, 2011.
- [19] M. Kanevski, Advanced Mapping of Environmental Data, Hoboken: John Wiley & Sons, 2008.

Appendix A – Training data

Sensor no.	Height [m]	Activity [1/s]				
		State 0	State 3	State 6	State 8	State 10
1	7.0	1000.0	3000.0	3000.0	3500.0	1000.0
2	6.5	2100.0	4500.0	4600.0	5100.0	5200.0
3	6.0	3000.0	5000.0	5600.0	6100.0	6200.0
4	5.5	3600.0	4600.0	6000.0	6100.0	6300.0
5	5.0	3900.0	4200.0	5850.0	6000.0	6100.0
6	4.5	4000.0	4000.0	5400.0	5600.0	5700.0
7	4.0	3900.0	3900.0	4800.0	5000.0	5100.0
8	3.5	3600.0	3600.0	4000.0	4200.0	4300.0
9	3.0	3000.0	3000.0	3100.0	3300.0	3400.0
10	2.5	2100.0	2100.0	2100.0	2200.0	2300.0
11	2.0	1000.0	1000.0	1000.0	1000.0	1100.0
12	1.5	0.0	0.0	0.0	0.0	100.0
13	1.0	0.0	0.0	0.0	0.0	0.0
14	0.5	0.0	0.0	0.0	0.0	0.0
15	0.0	0.0	0.0	0.0	0.0	0.0

Table A-1: Training data for development of models – numbers of states as used for training of the models (part 1/2)

Sensor no.	Height [m]	Activity [1/s]				
		State 11	State 13	State 15	State 16	State 18
1	7.0	1000.0	1000.0	1000.0	1000.0	1000.0
2	6.5	1500.0	1500.0	1500.0	1500.0	1500.0
3	6.0	1500.0	1500.0	1500.0	1500.0	1500.0
4	5.5	6100.0	1500.0	1500.0	1500.0	1500.0
5	5.0	7200.0	6800.0	1500.0	1500.0	1500.0
6	4.5	7500.0	7900.0	6800.0	1500.0	1500.0
7	4.0	7600.0	8200.0	7900.0	1500.0	1500.0
8	3.5	7800.0	8300.0	8200.0	1500.0	1500.0
9	3.0	7400.0	8700.0	8300.0	1500.0	1500.0
10	2.5	5900.0	8300.0	8700.0	1500.0	1500.0
11	2.0	2800.0	5800.0	8200.0	2500.0	2500.0
12	1.5	100.0	100.0	6400.0	8800.0	7500.0
13	1.0	0.0	0.0	2400.0	10000.0	10000.0
14	0.5	0.0	0.0	1700.0	8800.0	9500.0
15	0.0	0.0	0.0	1500.0	4000.0	6000.0

Table A-2: Training data for development of models – numbers of states as used for training of the models (part 2/2)

Appendix B – Test data

Sensor no.	Height [m]	Activity [1/s]				
		State 1	State 2	State 4	State 5	State 7
1	7.0	1600	2200	3000	3000.0	3250.0
2	6.5	2800	3900	4500	4550	4850.0
3	6.0	3700	4300	5200	5300	5850.0
4	5.5	4100	4200	4900	5500	6050.0
5	5.0	4050	4100	4500	5250	5925.0
6	4.5	4000.0	4000.0	4200.0	4800.0	5500.0
7	4.0	3900.0	3900.0	4100.0	4350.0	4900.0
8	3.5	3600.0	3600.0	3600.0	3700.0	4100.0
9	3.0	3000.0	3000.0	3000.0	3050.0	3200.0
10	2.5	2100.0	2100.0	2100.0	2100.0	2150.0
11	2.0	1000.0	1000.0	1000.0	1000.0	1000.0
12	1.5	0.0	0.0	0.0	0.0	0.0
13	1.0	0.0	0.0	0.0	0.0	0.0
14	0.5	0.0	0.0	0.0	0.0	0.0
15	0.0	0.0	0.0	0.0	0.0	0.0

Table B-1: Test data for development of the models – numbers of states as used for development of the models (part 1/2)

Sensor no.	Height [m]	Activity [1/s]			
		State 9	State 12	State 14	State 17
1	7.0	2250.0	1000.0	1000.0	1000.0
2	6.5	5150.0	1500.0	1500.0	1500.0
3	6.0	6150.0	1500.0	1500.0	1500.0
4	5.5	6200.0	3800.0	1500.0	1500.0
5	5.0	6050.0	7000.0	4150.0	1500.0
6	4.5	5650.0	7700.0	7350.0	1500.0
7	4.0	5050.0	7900.0	8050.0	1500.0
8	3.5	4250.0	8050.0	8250.0	1500.0
9	3.0	3350.0	8050.0	8500.0	1500.0
10	2.5	2250.0	7100.0	8500.0	1500.0
11	2.0	1050.0	4300.0	7000.0	2500.0
12	1.5	50.0	100.0	3250.0	8150.0
13	1.0	0.0	0.0	1200.0	10000.0
14	0.5	0.0	0.0	850.0	9150.0
15	0.0	0.0	0.0	750.0	5000.0

Table B-2: Test data for development of the models – numbers of states as used for development of the models (part 2/2)

Appendix C – Data-CD

Input datasets for all of the investigations, outputs of trainings of the models as well as the developed models are placed on the attached data-CD.

Folder *Data_R* contains all the input data for development, quality analysis and sensitivity analysis of both TSK models.

Folder *FM model* contains the fuzzy model by Mamdani (.fis, MATLAB 7.9.0), its results for recall dataset 3 and results for sensitivity analysis.

Folder *MLP models* contains all 20 trained MLPs (.mlp, DataEngine 4.0), their results for training-, test- and all three recall datasets, as well as input data and results of the models for the sensitivity analysis (for two best-choice models).

Folder *TSK models* contains 9 TSK n.n. models, 9 TSK n. models (in separated folders), results of their training, test, all three recalls and results of sensitivity analysis (of the best-choice models).

Original recall datasets (.xlsx, MS Excel 2007) are saved in the root folder of the data-CD, as well as a pdf of the thesis.